Accepted Manuscript

Quarterly Journal of Engineering Geology and Hydrogeology

A sensitivity analysis of a single extraction well from deep geothermal aquifers in the Cheshire Basin, UK

Christopher S. Brown, Nigel J. Cassidy, Stuart S. Egan & Dan Griffiths

DOI: https://doi.org/10.1144/qjegh2021-131

To access the most recent version of this article, please click the DOI URL in the line above. When citing this article please include the above DOI.

Received 16 September 2021
Revised 2 December 2021
Accepted 2 December 2021

A sensitivity analysis of a single extraction well from deep geothermal aquifers in the Cheshire Basin, UK

Christopher S. Brown[1,2*], Nigel J. Cassidy[2], Stuart S. Egan[3], Dan Griffiths[4]

Manuscript written for the journal Quarterly Journal of Engineering Geology and Hydrogeology

[1] James Watt School of Engineering, University of Glasgow, Glasgow, G12 8QQ.

* christopher.brown@glasgow.ac.uk

[2] Department of Civil Engineering, University of Birmingham, Edgbaston, Birmingham, B15 2TT, UK.

n.j.cassidy@bham.ac.uk

[3]Geography, Geology and the Environment, William Smith Building, Keele University, Keele, Staffordshire, ST5 5BG, UK. s.s.egan@keele.ac.uk

[4] Cheshire East Council, Westfields, Middlewich Road, Sandbach, CW11 1HZ.

Dan.Griffiths@cheshireeast.gov.uk

Abstract

Deep hot sedimentary aquifers (HSAs) are targeted for geothermal exploitation in the Cheshire Basin, UK. In this study, a single extraction well targeting the Collyhurst Sandstone Formation was modelled on MATLAB coupling heat and fluid flux. The Collyhurst Sandstone Formation in the Crewe area of the Cheshire Basin is expected to be found at a depth of 2.8 to 3.5 km, and was chosen as an area for geothermal exploration due to the high demand for energy.

Model results suggest that low-enthalpy, deep geothermal systems with thick HSAs are affected by both geological and engineering parameters. The results of this study highlight that the thermal gradient, hydraulic conductivity, production rate, length and position of the well screen are the key parameters capable of affecting the success and viability of any single well scheme. Poor planning during exploration and development can hinder the productivity of any single well scheme and these parameters must be considered to fully understand the risk. Engineering parameters, such as the length of the well screen, can be used during well planning to mitigate geological risks in the aquifer, whilst the results presented can also be used as a guide for energy potential under varying conditions.

1. Introduction

In the UK, there is a growing demand for clean, CO_2 neutral, renewable energy sources to replace fossil fuels. Deep hot sedimentary aquifers (HSAs) hold the potential to be exploited for low-

enthalpy geothermal energy, meeting part of the growing energy demand. There are four major Mesozoic sedimentary basins in England and Wales considered to have the potential to yield low-enthalpy, geothermal resources from HSAs, including; the Worcester, East England, Wessex and Cheshire Basins (Busby, 2010, 2014) (Fig. 1). In recent years there has been a renewed drive for geothermal energy in the UK (e.g., Mannin et al., 2007; Younger et al., 2010; Younger et al., 2016; Gluyas et al., 2018; Westaway, 2018; Watson et al., 2019; Brown et al., 2021; Howell et al., 2021; Watson et al., 2021). Yet, currently, the only HSA deep geothermal resource being developed is at Southampton in the Wessex Basin, with a single well scheme targeting the Sherwood Sandstone Group (SSG) for district heating, supplying over 3000 buildings (Barker et al., 2000; Lund et al., 2011).

The single well scheme in Southampton is unique, as it only uses one well and not the typical doublet configuration most low-enthalpy geothermal systems use. The single well produces 74 °C fluid at 10-15 l/s and contributes 18 % of the energy to a combined heat and power (CHP) 5.7 MW district heating plant (Smith, 2000, Energie-Cités, 2001). Saline fluid passes through a heat exchanger, before being discharged into the sea (Energie-Cités, 2001). As the well has been used to provide renewable energy for over 30 years without the need for a re-injection well, this paper aims to test whether the use of single wells is replicable across the UK, with a view they can produce energy for district heat networks without the need for significant initial capital expenditure that doublet schemes incur. Although we investigate the hypothetical aquifer response and longevity of the resource under extraction conditions, wastewater disposal is not considered. The disposal of the extracted geothermal brine in single well schemes remains a key issue during development. In areas inland, where the option to dispose into the sea is not possible, fluid may be discharged to the subsurface via a shallow well (or direct infiltration from ground level where geology permits) after passive or active treatment for chemicals and desalination (e.g., Westaway, 2018). Such a discharge would likely require a permit under the Environmental Permitting (England & Wales) Regulations 2016 and proves to pose a major risk on development.

Mesozoic basins in the UK (Fig. 1) hold an estimated total resource of 327 EJ (Rollin et al., 1995), with c. 23% (~ 75 EJ) of this estimated to be untapped within the Cheshire Basin (Rollin et al., 1995; Hirst et al., 2015). A preliminary study after the oil crisis of the 1970s (e.g., Barker et al., 2000) made initial estimates of both the energy and the quality of potential geothermal aquifers (Downing and Gray, 1986) without any schemes in the basin being developed commercially. In this study, an explicit numerical model is developed, investigating the production of hot water from the Collyhurst Sandstone Formation based on a single extraction well under varying geological and engineering scenarios. Permian aeolian to -fluvial sandstones buried at depths of 2.8 - 3.5 km were investigated (Fig. 2 & 3) due to their favourable temperatures (up to 100 °C) (Downing and Gray, 1986; Barker et al., 2000; Busby, 2010, 2014). The low-enthalpy energy in the Mesozoic rocks in the Cheshire Basin and older Palaeozoic rocks is likely to be used for direct heat use including balneology and district heating, thus to limit heat loss, the distribution of the UK's population is likely to dictate the development of any geothermal scheme. For this reason, the subsurface underlying the Crewe area (Cheshire, UK) is investigated (Fig. 3a). The Crewe area is also located in the centre of the basin with the highest geothermal resource expected to be concentrated around the deepest parts of the aquifer. The modelled data can be used to aid future geothermal-district heating schemes in the area providing planners with the information needed to match supply and demand. Furthermore, recent studies have planned for a multi-phase district heat network plan in Crewe (Cheshire, UK), aiming to gradually increase the energy supply to businesses in the town centre, eventually reaching a peak demand of 35 MW, or 76 GWh/year (Routledge et al., 2014).

Currently, few wells penetrating depths of 3 km have been drilled in the Cheshire Basin, meaning that the quality, extent and temperatures of HSAs in this region are unknown. The lifetime of a well targeting low-enthalpy HSAs is controlled by both geological and engineering parameters, including (for doublet schemes) porosity, pore fluid salinity, initial aquifer temperature and extraction rate, respectively (Saeid et al., 2015). In this study, a preliminary parametric study is presented that investigates the exploitation of energy under varying geological and engineering

conditions for a single well scheme for the first time. The aim of the study is to help identify and mitigate the risks associated with the varying hydraulic and thermal conditions at depth for single well schemes, particularly those with thick HSAs. Regression analysis shows trends in the production data, whilst K-means cluster analysis is used to group the production data and has been used to determine the risk in relation to pre-set cut-offs. The geological factors investigated include aquifer thickness, hydraulic conductivity, thermal gradient, thermal conductivity of the aquifer and porosity. The engineering parameters investigated were production rate, borehole radius, length of the well screen and position of the well screen. The wellbore material was not investigated as it has a minimal effect on the lifetime of a geothermal system, only affecting the initial production temperature (Saeid et al., 2015).

The geothermal system was modelled with MATLAB software, using the finite-difference method that couples both convective and conductive heat transfer (Fig. 2a). Although the aquifer and surrounding confining beds were modelled in 3D, the wellbore was simulated in 1D. The wellbore model is based on that of Al-Khoury et al. (2005) and Al-Khoury and Bonnier (2006), with further development by Saied et al. (2013) and Brown et al. (2021). The 1D wellbore reduces the nodal quantity used, saving computational time. The 1D wellbore is extremely important to model as it can give an accurate estimate of the production temperature. If the production temperature is assumed to be that of the sink points in the aquifer then a significant part of the geothermal system is neglected giving inaccurate results, likely to be over predicting the thermal energy produced as losses in the wellbore are neglected. The use of a 1D wellbore also reduces the need for modelling complex geometries, which can be particularly problematic when using the finite-difference method.

Currently, the geological risks of any geothermal scheme in the Cheshire Basin are too high for investors and plans to develop geothermal energy in the Crewe area are in their infancy. This study aims to bridge this gap by presenting realistic results for a single well scheme under varying geological and engineering parameters, highlighting the key areas of risk in the basin and how they

can be mitigated. This is vital for decision makers in the local authorities who are looking to exploit the energy through a district heat network. The results are also of importance to other low-enthalpy, single well geothermal schemes targeting thick aquifers, stressing the importance of key characteristics to well engineers.

2. Geological Setting

The Cheshire Basin is one of a series of Permo-Triassic extensional sedimentary basins located across the UK (Fig. 1) associated with the rifting of Pangaea and the breakup of Laurasia (Glennie, 1995; Rowley and White, 1998). Extensional collapse occurred after the Variscan orogeny resulting in tilted fault blocks and graben structures (Figs. 3b & 3c) (Ruffell and Shelton, 1999). The Cheshire Basin has a thick succession of infill consisting of high-quality Permo-Triassic sandstone aquifers (Sherwood Sandstone and Appleby Groups) overlain by the confining and thermally insulating mudstone sequence (Mercia Mudstone Group) (Fig. 3a & c). The Permo-Triassic sandstones have been characterised thoroughly, retaining high micro-porosity at depth (e.g., Allen et al., 1985, 1997; Downing and Gray, 1986; Griffiths et al., 2003; Ambrose et al., 2014). The most basal member and target of deep geothermal extraction in this model is the Collyhurst Sandstone Formation of the Appleby Group. The Collyhurst Sandstone Formation is an arenaceous, aeolian- to fluvial-sandstone with core data showing high porosities (13-32%) and hydraulic conductivities (<10 m/d or ~4.5e-12 m^2) (Allen et al., 1997). The formation is overlain by the Manchester Marl Formation, which is anticipated to be a confining, low-permeability seal that was deposited during a marine incursion in the mid-Permian (Naylor et al., 1989). The Manchester Marl Formation is composed of mudstones intercalated with limestones becoming siltier and thinner to the south of the basin (Evans et al., 1993). As a result, the formation is considered a confining seal preventing hydraulic continuity between the Collyhurst Sandstone Formation and Sherwood Sandstone Group.

Carboniferous strata directly underlie the basal Permian sandstones and are predominantly fluvial, to semi- to open-marine in depositional environment. Marls, sandstones, limestones, coals

and shales have all been identified in outcrop studies (e.g., Gibson, 1901; Smith, 1998; Powell et al., 2000). Early Carboniferous strata are deposited in a marine setting followed by a fluvial to lacustrine setting, representing a shallowing-upwards sequence, associated with uplift during the Variscan orogeny. The lateral extent of the Upper Carboniferous strata underlying the Cheshire Basin has been widely debated with some suggesting that in the deep, south-eastern part of the basin basal Permian sandstones lie directly on low-grade metamorphic Palaeozoic rocks (Fig. 3c – with potential Carboniferous strata extent hypothesised) (Abdoh et al., 1990; Mikkelsen and Floodpage, 1997). This is due to fault reactivation during the Variscan orogeny uplifting Carboniferous strata in the south of the basin (Fig. 3b). Although this could limit the thickness of the geothermal resource at higher temperatures, thick outcrop successions of Carboniferous strata in the east indicate the opposite (Hirst et al., 2015). In this study, both scenarios are considered; (1) the Collyhurst Sandstone Formation lies directly on low-grade metamorphic rocks, acting as an impermeable seal and (2) the Collyhurst Sandstone Formation overlies the Warwickshire group – a thin succession of Carboniferous sandstone (Salop and Halesowen Formations) underlain by a bottom seal (Etruria Marl formation/low-grade metamorphic basement). Although the Salop and Halesowen Formations are far more lithologically complex and heterogeneous, they are considered as an extension to the aquifer with the same properties (extension to aquifer thickness). To understand the effects of the parameterisation of engineering and geological properties, the former scenario is used as a base case.

3. Methodology

3.1 Governing equations of the aquifer and wellbore

The finite-difference method was used to model the aquifer and wellbore, coupling heat transfer and fluid flow. The orthogonal mesh was discretised on a non-uniform grid with fixed Cartesian co-ordinates (Fig. 2a). The model assumes the aquifer is initially fully saturated and the pressure head is equal to the depth. It is unlikely that the aquifer will be fully screened for an

interval of ~700 m; it was therefore assumed that the wellbore will be screened for an interval of 70 m in the base case. An axis-symmetric model was used for faster computational time. The varying effects of penetration ratio were also investigated.

The governing equations used for the aquifer model both heat transfer and fluid flow. Both the solid and fluid components (subscript s and f respectively; symbols listed in the nomenclature) can be modelled to give the advection-diffusion equation (e.g., Saeid et al., 2013):

$$\frac{\partial T}{\partial t} = -R_d.\mathrm{v}.\nabla \mathrm{T} + \alpha_b \nabla^2 \mathrm{T} \qquad 1$$

where R_d is a retardation factor, which represents the change of temperature based on the specific heat capacity for the system.

$$R_d = \frac{\rho_f C_f}{(1-\emptyset)\rho_s C_s + \emptyset \rho_f C_f} \qquad 2$$

The bulk thermal diffusivity (α_b) is the sum of the solid and fluid phases:

$$\alpha_b = \frac{\lambda_b}{\rho_b C_b} = \frac{(1-\emptyset)\lambda_s + \emptyset \lambda_f}{(1-\emptyset)\rho_s C_s + \emptyset \rho_f C_f} \qquad 3$$

where λ is the thermal conductivity, T is the temperature, v is the Darcy velocity, $\emptyset$ is the porosity, ρ is the density and C is the specific heat capacity. Darcys Law can be used to calculate the fluid velocity $v = -K(\nabla h)$, where the hydraulic head is h and the hydraulic conductivity is K. Although numerical diffusion can pose problems in advective finite-difference schemes (Wu et al., 2019), it is avoided in this study by ensuring the mesh is refined around high temperature contrasts (i.e., the wellbore) and monitored by comparing the numerical solution against an analytical solution.

The continuity equation is expressed as the change of head with respect to the Darcy velocity and can be derived assuming the fluid is constant and the rock is non-deformable (i.e., porosity is constant) (e.g., Rushton, 2003; Sachse et al., 2015):

$$\rho\frac{\partial\emptyset}{\partial t}+\ \rho\nabla(\emptyset V)=W \qquad 4$$

where $V$is the average velocity and W is a sink or source. Dividing the continuity equation by the density (ρ) gives:

$$\frac{\partial\emptyset}{\partial t}+\ \nabla(\emptyset V)=\frac{W}{\rho} \qquad 5$$

which can be modelled for hydraulic head as (Anderson et al., 2015):

$$S_s\frac{\partial(h)}{\partial t}+\ \nabla\cdot(v)=W \qquad 6$$

where storativity is S_s.

The thermal interactions between the wellbore and surrounding rocks were modelled using a 1D scheme developed by Al-Khoury et al. (2005) and Al-Khoury and Bonnier (2006) for shallow geothermal systems and adapted by Saeid et al., (2013) for deep geothermal systems (Fig. 2b).

$$\rho_f C_f\frac{\partial T_p}{\partial t}A_p-\lambda_f\frac{\partial^2 T_p}{\partial z^2}A_p+\rho_f C_f u_p\frac{\partial T_p}{\partial z}A_p=b_{pg}(T_g-T_p)2\pi r_p \qquad 7$$

$$\rho_g C_g\frac{\partial T_g}{\partial t}A_g-\lambda_g\frac{\partial^2 T_g}{\partial z^2}A_g=b_{pg}(T_p-T_g)2\pi r_p+b_{sg}(T_s-T_g)2\pi r_g \qquad 8$$

$$\rho_s C_s\frac{\partial T_s}{\partial t}A_s-\lambda_s\frac{\partial^2 T_s}{\partial z^2}A_s=b_{sg}(T_g-T_s)2\pi r_g \qquad 9$$

The subscript g is the respective property of the grout, whilst p is for the pipe and s is the solid rock surrounding the well. The thermal conductivity is λ, the specific heat capacity is C, the density is ρ, the fluid velocity is u_p, the area of the grout is A_g, the reciprocal of thermal resistance between the wellbore pipe and grout is b_{pg}, the reciprocal of the contact resistance between the grout and soil is b_{sg} etc.

Head in the wellbore can be modelled as (e.g., Halford and Hansen, 2002; Konikow et al., 2009):

$$h_w = h - \left(\frac{Q}{2\pi Kb}\ln\left(\frac{r_e}{r_w}\right)\right) - \Delta h_p \quad (10)$$

The well head (h_w) can be calculated by subtracting the change in head in the wellbore under fully penetrating conditions (using the Thiem equation; Δh_t) and the change in head caused by partial penetration effects (Δh_p) (Thiem, 1906; Kozeny, 1933; Pricket, 1967). The production rate (Q) is then calculated as ($W = \frac{Q}{\Delta x.\Delta y}$), the thickness of the aquifer is b and the wellbore radius is r_w.

The effective radius (r_e) is calculated as ($r_e = \frac{\Delta x}{4.81}$) where $\Delta x = \Delta y$ and is equivalent to the radius of a vertical pumping well for the node of the cell (Fig. 4) (e.g., Pricket, 1967; Peaceman, 1983). The Thiem equation can be used to approximate the head in the well which will usually be lower than the effective radius. This method follows multiple assumptions: the aquifer is confined, the well is vertical and the screened section penetrates the full cell, drawdown is symmetrical radially, flow in the cell containing the well is only radial, the time period used to solve the head in the well is steady state and there is homogenous strata around the well with a constant hydraulic conductivity (e.g., Konikow et al., 2009). Change in head from partial penetration can be calculated as (Kozeny, 1933; Prickett, 1967):

$$\frac{\Delta h_p}{\Delta h_t} = PC = \frac{1}{Pr\left[1+7\sqrt{\frac{r_w}{2bPr}}\cos\left(\frac{\pi Pr}{2}\right)\right]} - 1 \quad (11)$$

where Pr is the penetration ratio.

The mass flow rate is applied as a sink (W) divided equally across the well screen nodes in the aquifer. At this interface the wellhead in the wellbore can be calculated using the average head across the well screen nodes evaluated at each time step. The 1D wellbore is coupled to the aquifer by setting the base to be equal to that of the average temperature across nodes formulating the well screen (Saeid et al., 2013), whilst the production temperature is recorded at the top of the wellbore.

When solving the governing equations for heat flux the wellbore is simulated as a 1D nodal line within the discretised 3D geological model. The 1D wellbore line component is solved by simulating heat flux horizontally using thermal resistance and vertically using the finite-difference method (Eqs. 7-9). The 3D mesh is then solved in 3D using the finite difference method for both heat and fluid flux (Eqs. 1 & 6).

3.2 Energy production

To assess the economic viability for any geothermal scheme the total quantity of energy produced must be determined. For a single well scheme the total energy production (E_{prod}) can be calculated as (modified from Crooijmans et al., 2016 for a single well scheme):

$$E_{prod} = \sum_{t=1}^{n} Q.\Delta t.c_f \rho_f.(T_{prod} - T_{rej}) \quad 12$$

where n is the number of time steps, Δt is the time step, T_{prod} is the production temperature and T_{rej} is the rejection temperature. For this study, it is assumed that the rejection temperature, where the water is deemed no longer suitable for a district heating scheme, is 30 °C. The rejection temperature is the lowest value that can be used in a heat network and is in line with that proposed by other authors for the Cheshire Basin (e.g., Downing and Gray, 1986). It is, however, worth noting that further heat can be extracted from waters under 30°C using heat pumps and be used as a low temperature resource, such as in mine water systems (e.g., Verhoeven et al., 2014; Farr et al., 2021)).

3.3 Discretisation, boundary and initial conditions

The model was discretised using an orthogonal mesh with the spacing expanding horizontally away from the wellbore using an expansion factor of 1.2 to 1.5, with the spacing around the well of 8 m. In the aquifer, thermal and fluid fluxes were modelled explicitly, whilst heat fluxes in the wellbore were modelled using an implicit-explicit (IMEX) operator splitting procedure (e.g., Spiegelman, 2000; Geiser, 2008) where the diffusion component of Eq. 7 is modelled explicitly,

whilst the convective component is then modelled implicitly. This procedure allows a greater range of time steps to be used for the wellbore and increased stability. This method of wellbore modelling retains accuracy, with results identical to the purely explicit method, both spatially and temporally. Computational time when modelling heat flux in the wellbore is dramatically reduced, however, the time step size must still be considered carefully to ensure accuracy is maintained.

The effect of lateral boundaries is designed to be insignificant by extending the horizontal domain of the model to minimise thermal and hydraulic interactions. Boundary interactions were monitored during the simulations with thermal and hydraulic propagation around the borehole always less than 3 km. The lateral boundaries were all set as fixed constant temperatures/heads. The confining boundaries above and below the aquifer were set as no flow boundary conditions for fluid flow. The base of the model was set at a fixed constant temperature, whilst the surface level boundary is set to have no heat flux.

Under initial conditions the model is set up using a linear gradient for temperature:

$$T_{(z)} = T_{(0)} + \Delta T.z \qquad 13$$

with the surface temperature ($T_{(0)}$) set to 10 °C (BGS, 2011). The initial hydraulic head in the wellbore was set to 3500 m, the porosity was set to 15%, the production rate to 15 l/s, the hydraulic conductivity as 0.1 m/d (4.6e-14 m^2 equivalent permeability) and the storativity as 4e-4 which is in-line with deep confined aquifers within the basin (pump tests and modelled (Allen et al, 1997; Cai and Ofterdinger, 2014)) (Table 1). The hydraulic conductivity was chosen slightly lower than the geometric mean (0.4 m/d) to reflect further reduction in permeability as few wells in the Cheshire Basin reach the depths targeted here. The hydraulic conductivity and porosity of the confining upper seal (Manchester Marl Formation) and lower confining beds (considered to be low-grade metamorphic rock (Abdoh et al., 1990; Mikkelsen and Floodpage, 1997; Hirst et al., 2015)) was set equal to zero. There is debate on the nature of the Manchester Marl Formation; regarding whether

it is likely to be an aquitard or seal. In this study, it was considered an impermeable seal for several reasons, including: 1) fluid propagation around the well is predominantly radial and vertical fluxes are likely to have minimal impact, 2) the Manchester Marl Formation lacks data at depth particularly in the central part of the basin, 3) the Manchester Marl Formation acts as a seal in hydrocarbon fields (e.g., Pharaoh et al., 2019) 4) literature regards the Manchester Marl Formation as largely impermeable with local low-permeability zones (University of Birmingham, 1984; Griffiths et al., 2005), 5) permeability will reduce with depth and 6) computational time can be saved by imposing an impermeable layer rather than a low-permeability seal. It should, however, be noted that in reality the complex geological lateral variations in this stratigraphic unit could influence any geothermal developments and requires further geological assessment.

The thermal conductivity was set to 3.41 W/m/°C in the aquifer and 2.12 W/m/°C for the upper confining beds (Downing and Gray, 1986). The heat capacity was set to 950 J/kg °C for the upper confining beds and 775 J/kg °C for the aquifer, whilst the density was set to 2450 kg/m^3 for the aquifer, 2720 kg/m^3 for the upper the confining beds (Waples and Waples, 2004). The fluid salinity was set at 80 g/l (similar to that of modelling from Plant et al. (1999) and that of the Southampton geothermal fluid (Downing and Gray, 1986)), with a specific heat capacity of 4200 J/kg °C (ETB, 2017) and a conductivity of 0.67 W/m/°C (Ozbek and Phillips, 1979)). The density of the fluid was set as a constant using the initial aquifer temperature and salinity, calculated as 1024.7 kg/m^3 (Batzle and Wang, 1992; Adams and Bachu, 2002; Saied et al., 2015; Crooijmans et al., 2016).

For the base case, the wellbore has the following parameters (Table 2): a well screen radius of 0.106 m, piping thermal conductivity of 43 W/m/°C, grout thermal conductivity of 2.7 W/m/°C, grout specific heat capacity of 1250 J/kg °C, grout density of 1600 kg/m^3, pipe thickness of 0.02 m and grout thickness of 0.04 m (Price and Allen, 1984; Allan 1997; ETB 2017; Rosen and Koohi-Fayegh, 2017). The radius of the piping in the wellbore was modelled at 0.153 m to match that of Southampton (Downing et al. 1984). Simulations were run for 25 years.

The lifetime of a well was determined by analysing the production temperature and head in the wellbore. Cut-offs were set for when head in the wellbore is less than 3000 m or production temperature is less than 60 °C. In comparison to the initial conditions this is a drawdown of 500 m and was chosen to match that of the submersible pump used in Southampton. This was submersed to 617 m below the datum and capable of dealing with high temperatures (Price and Allen, 1984). Under static conditions the production temperature is equal to the surface temperature (10 °C), however, after production starts the temperature rapidly reaches above 75 °C. Therefore, for production temperature the cut-off is set after the initial heating phase and typically occurs due to change of initial aquifer temperature (e.g., due to reduced thermal gradient).

3.4 Model Benchmarking

The model was compared to two analytical solutions; the first a modified version of the Theis solution (Brons and Marting, 1961; Hantush, 1961, 1962; Huisman, 1972; Sternberg, 1973) and the second an analytical solution for advection-diffusion developed by van Genuchten and Alves (1982). Both analytical solutions were chosen to test the model accuracy of the hydraulic head in the well and the production temperature, respectively, over the lifetime of a simulation (25 years). The parameters used were identical to the base case; however, the analytical solution for heat flow requires a new thermal resistance between the pipe and surrounding rock in the absence of the grout. This was calculated as 30 W/m/°C. When comparing to the Theis solution the well screen was modelled in the centre of the aquifer.

When comparing the numerical and analytical models for fluid flow (Fig. 5), initially the difference in drawdown was higher in the first 10 days, however, the difference is then minimal (<2 %) and both solutions trend together closely for the remainder of the simulation (Fig. 5). As we are interested in changes in head over the lifetime of a geothermal system under exploitation for 25 years, the initial loss in accuracy is deemed acceptable. The end difference in solutions was 0.026 % and 0.05 m head (Fig. 5).

When testing for thermal changes some numerical modelling simplifications were made to match the analytical solution: 1) no grout is present in the wellbore, 2) the outer rock is a constant temperature which does not change and 3) the surrounding rock is the average temperature from the surface to the base of the wellbore (45 °C). The analytical and numerical solutions match extremely closely. During the simulation, the numerical solution's production temperature was always slightly elevated in comparison to the analytical solution (Fig. 6a) and at the end of the 25 year simulation the top of the wellbore is within 0.06 °C of the analytical solution (Fig. 6b). The max MAPE was also highest at the surface level, however is still relatively low at 0.075 % (Fig. 6b). Further benchmarking for the 1D wellbore component can be found in Brown et al. (2021), whilst Howell et al. (2021) and Brown (2020) show further benchmarks for the 3D geological media.

3.5 Parameterisation

Multiple parameters were modelled in a localised sensitivity analysis to account for both geological and engineering conditions for the Cheshire Basin (Table. 3). Porosity was modelled at 10 %, 20 % and 30 %, which reflects the range of potential porosities of the Collyhurst Sandstone Formation (Allen et al., 1997). These values are similar to that of offshore analogues in the East Irish Sea Basin where porosity values range from 5-25% for the Collyhurst Sandstone Formation (e.g., Hirst, 2017). Thermal conductivity of the Collyhurst Sandstone Formation was modelled at 2 W/m/°C, 4 W/m/°C and 5 W/m/°C, which is similar to Permo-Triassic rocks across the UK (Downing and Gray, 1986). The thickness of the Collyhurst Sandstone Formation is poorly constrained on seismic data under the deepest parts of the Cheshire Basin, with few wells penetrating over 3 km in the basin. Thickness variations of -70, +140 and +70 m were considered (thickness added at the base of the aquifer). Hydraulic conductivity was modelled for three scenarios, with all values less than the base case scenario to test the influence of poorer hydraulic conductivity. Core data studies within the basin indicate hydraulic conductivities are between 3.7×10^{-5} and 10 m/d, with a mean of 0.4 m/d (Allen et al., 1997). It is, however, anticipated that porosity and permeability will decrease

with depth, such that flow rates will be lower the deeper they are. Therefore, hydraulic conductivities lower than these were modelled: 0.01 m/d, 0.03 m/d and 0.05 m/d ((4.76e-15 m^2, 1.39e-14 m^2 and 2.3e-14 m^2 equivalent permeability, respectively). Further consideration was also given to other hydraulic conductivities that reflect analogous offshore data in the East Irish Sea Basin which range from ~0.0001 m/d to ~0.5 m/day (Hirst, 2017). Additionally, a variety of thermal regimes were modelled to reflect the literature between 17 - 28 °C/ km (Downing and Gray, 1986; Busby et al., 2011; Atkins, 2013).

The position of the well screen can be important to the depletion of fluid in the aquifer as the confining upper or lower boundary can reduce the proximal quantity of fluid that can be drawn into the wellbore. The three scenarios investigated locate the wellbore in the upper middle, lower middle and base of the aquifer (Table 3). Production rate from the Collyhurst Sandstone Formation was modelled for rates of 20-40 l/s (Griffiths et al., 2003; Atkins, 2013). A range of well screen lengths were modelled including fully penetrative in the aquifer, partially penetrative at 280 m length and 140 m length. To investigate the effects of a slim borehole versus regular borehole, a range of well radii were used (0.05 – 0.02 m).

4. Results

4.1 Base case

As the base case thickness of the aquifer was set to 700 m, it is expected that temperature will be hotter towards the base, using a linear relationship between increasing temperature and depth under static conditions. The well screen was located at the top of the aquifer and has a penetration ratio of 10% (parameters summarised in table 1 and 2). With time, the hot water front at the base of the aquifer was pulled upwards towards the well screen, increasing the production temperature and decreasing the head at the well screen in the HSA (Fig. 7a). Vertical fluxes within the wellbore were most significant, with minimal temperature change in the aquifer and confining beds (Fig. 7). During

production, over the lifetime of a single well (25 years), the head decreased by 200.2 m and the temperature at the well screen increased by 1.895 °C (solid red line labelled 'aquifer temperature' in Fig. 7b).

During the lifetime of the well 11,826,000,000 litres of water were produced which is equivalent to 2.37×10^{15} Joules of energy. This is based on the assumption that production temperature is recorded at the top of the production well, otherwise if aquifer temperature is used the energy produced is over-estimated at 2.59×10^{15} Joules. The zone of influence around the well within the HSA reached a maximum radius of 2.285 km, covering an area of 16.4 km^2 (taken at the middle of the length of the well screen, to 1m of the static HSAs head). The greatest difference in temperature was constrained to near the well screen (within ~200 m) (Fig. 7a).

Temperature distribution along the wellbore piping rapidly changed in the first 5 days, immediately increasing in the first 6 hours such that the temperature along the wellbore exceeded 25 °C (Fig. 7c). In the confining strata (i.e., the overburden above the aquifer), thermal propagation away from the hot borehole was minimal, and radially only reached a distance of 50 m at the end of the simulation (Fig. 7d). Within the first year, temperature in the pipe and grout were similar at 75.46 °C and 75.01°C respectively, whilst the temperature in the confining rock was slightly lower by 2.16 °C. At the end of production there was a 3.7 °C loss in temperature within the wellbore (between well screen and surface level). At the end of the 25 year lifetime, the temperature at: the well screen interval was 82.77 °C, the confining rocks around the wellbore at surface level was 77.13 °C, the grout at surface level was 78.74 °C and the production temperature at surface level was 79.07 °C. The small increase in production temperature (Fig. 7b) was due to a slight warming at the well screen due to the up-welling of warm water from the base of the aquifer and also the heating of the surrounding rock around the borehole during production. The heat load at the end of the simulation was recorded at 3.17 MW.

4.2 Parameterisation of the geological conditions

In order to understand the risks of varying geological conditions at depths, the model was used to test five geological parameters, including both hydro- and thermo-physical characteristics within the aquifer (Table 3). The effects on drawdown, production temperature, energy production and zone of influence were investigated to access which parameters are critical to the viability of any single well scheme. The base case showed a rapid change in head and production temperature within the first few hundred days, however the rate of change after this was minimal. As a result the end heads and production temperatures were compared to the base case for each parametric scenario.

4.2.1 Porosity

Porosity was modelled at 10 %, 20 % and 30 %. In the numerical model porosity only affects the thermal component and a linear relationship was observed between increasing porosity and decreasing temperature at the end of the simulations (Fig. 8a). As a result, porosity only has a minor effect with the temperature difference between minimum and maximum porosities observed with a difference of 0.13 °C, which equates to a difference of 4.8 TJ of cumulative energy during the simulations.

4.2.2 Thermal conductivity

Thermal conductivity values of the Collyhurst Sandstone Formation were investigated at 2 W/m/°C, 4 W/m/°C and 5 W/m/°C. Although this is an extreme range it reflects the lithological variations accounted for in literature (Downing and Gray, 1986). The range in thermal conductivity modelled had a minor effect on the production temperature at the end of the simulation. As shown in figure 8b, higher thermal conductivities have a logarithmic relationship with production temperature. Similarly, thermal conductivities have a minor effect on the achievable heat load, or total energy produced during the simulation. The production temperature at the end of the

simulation decreased from 79.11 to 79.03 °C, whilst the difference in total cumulative energy during the simulation was 2.1 TJ.

4.2.3 Aquifer thickness

The thickness of the Collyhurst Sandstone Formation was modelled for variations of -70, +70 and +140 m. An increase in the aquifer thickness resulted in an increase in production temperature, with the regression model showing a polynomial fit at the end of the simulation (Fig. 8c). The difference in temperature between the smallest and largest aquifer thickness was 0.013 °C. When considering the effect on head a 2 m difference between the thinnest and thickest aquifer was observed with a linear relationship. Although it appears that the aquifer thickness has a minor effect it should not be ignored completely in well planning when the hydraulic conductivity is unknown. It does play a key role in distinguishing the zone of influence; thinner aquifers cause an increase in the radius around the well screen that fluid is drawn in from. For the thinnest aquifer the radius that fluid was drawn in from was 2.735 km, whilst the thickest aquifer model has a final radius for the zone of influence of 2.06 km. It is also worth noting that the thickness affects the transmissivity of an aquifer and may have a more significant effect when the hydraulic conductivity is poor.

4.2.4 Thermal gradient

Thermal gradients were investigated between 17-28 °C. Thermal gradients alter the initial aquifer temperature and, therefore, can create a huge difference in production temperatures. At the end of the simulations a linear increase in production temperature was observed with increasing thermal gradients (Fig. 8d). A similar trend was observed in the cumulative energy production over the lifetime of the system. When the gradient was 17 °C/km the production temperature did not reach the 60 °C cut-off required for the district heating scheme and was unsuitable for production. In contrast elevated production temperatures and total energy produced were attained for the 28

°C/km thermal gradient. The maximum and minimum heat load produced for the highest and lowest thermal gradients was 3.71 and 1.745 MW, respectively.

4.2.5 Hydraulic conductivity

Hydraulic conductivity was modelled for three scenarios 0.01 m/d, 0.03 m/d and 0.05 m/d. Hydraulic conductivity had a minor effect on production temperature, with higher hydraulic conductivities resulting in an increase of temperature at the end of the simulations with a logarithmic fit (Fig. 9). Similarly, the head in the wellbore at the end of the simulations showed an increase of head with higher hydraulic conductivities with a logarithmic fit (Fig. 9). The effect on head was significant with a huge increase in drawdown observed for lower hydraulic conductivities. Low hydraulic conductivities resulted in rapid head drops in the aquifer around the wellbore, with the lowest hydraulic conductivity modelled resulting in the well head immediately dropping below the cut-off. Similarly, when modelling for a value of 0.03 m/day head dropped below the cut-off within the first few days of production. The zone of influence increased with greater conductivities, but the cone of depression was larger around the well screen for poorer hydraulic conductivities. The cone of depression increasing with lower hydraulic conductivities highlighted that head drop around the wellbore was rapid and fluid flux radially towards the well screen was not sufficient to replenish the extracted fluid. Although changing hydraulic conductivity only had a minor influence on energy output and production temperature, the key issue is that it may reduce inflow into the well such that drawdown in the well is too significant to produce water from, resulting in a reduced lifetime.

Further analysis was also undertaken to consider the analogue of the offshore East Irish Sea Basin, where hydraulic conductivities taken at depth range from ~0.0001 m/day to ~0.5 m/day (Hirst, 2017). Both of these values were simulated to understand the impact of hydraulic conductivity over a greater range which can be over several orders of magnitude. The minimum value simulated causes the model to immediately reduce lower than the cut-offs stated. In fact,

when applying the Thiem equation (Eq. 10) the steady state drawdown is calculated to be in excess of 3000 m implying that the well is dry and in reality no fluid would be produced. In contrast, the higher hydraulic conductivity gives minimal drawdown and the final head was recorded at 3458.9 m. Similarly to the other simulations for hydraulic conductivity the impact on production temperature was minimal.

4.3 Parameterisation of engineering conditions

Engineering components of a geothermal scheme may also have a positive or negative effect on aquifer response and energy production. Parameters such as production rate, wellbore radius, well screen length and well screen position were investigated to understand the most prominent well-design characteristic in influencing aquifer lifetime, temperature change, drawdown and energy production. Wellbore materials were not investigated as it has been proven that they have minimal effect on production (Saeid et al., 2015).

4.3.1 Position of well screen

The position of the well screen was modelled in the upper middle, lower middle and base of the aquifer (Table 3). The well screen position caused a linear increase in production temperature corresponding to the well screen being located at depth, directly correlating to the linear relationship between temperature and depth (Fig. 10a). Locating the well screen at the base of the aquifer instead of the top created an increase in the production temperature of 11 °C (observed at the end of the simulation). This had significant ramifications for the total energy produced, which increased due to the higher temperatures (Fig. 10b). The total energy produced over the simulation increased to 2.95 x 10^{15} J. When the well screen was not located toward the centre of the aquifer the interaction with upper and lower aquifer boundaries created an increase in drawdown by 14.2 m; this was observed with a polynomial fit (Fig. 10a).

4.3.2 Production rate

Production rates were modelled from 20 – 40 l/s and had an observed logarithmic increase with production temperature (Fig. 10c). Final production temperature increased by 3.3°C between the lowest and highest flow rate. The increase in quantity of fluid extracted and higher temperature production fluids resulted in a major impact on energy production (Fig. 10b). A maximum heat load of 9.03 MW was achieved for the 40 l/s flow rate, whilst the total energy produced during the simulation was 6.76×10^{15} J. Although the increase in fluid production rate has a clear benefit due to higher heat loads, it does have a negative that can be an obstacle to development due to decreasing wellbore heads. A linear relationship was observed, with the flow rate of 40 l/s meeting the cut-off for extraction due to the well head being too low to be drawn from (Fig. 10c). Higher flow rates may also be unsustainable as the zone of influence of a well significantly increased with greater production rates, leading to potential hydraulic interactions with lateral boundary conditions in more complex aquifers. The lowest flow rate had a zone of influence of 2.51 km, whilst the highest was 3.063 km.

4.3.3 Length of well screen

A range of well screen lengths were modelled including fully penetrative in the aquifer, partially penetrative at 280 m length and 140 m length. The length of the well screen plays an important role in controlling the drawdown in the aquifer. Increasing the well screen had a logarithmic relationship with increasing well head at the end of the simulation (Fig. 11a). Therefore, better performance can be expected with larger screened intervals; however, this will incur a greater cost. An increase in the well screen length also had a positive effect on production temperatures (Fig. 11a); this was due to water at depth being drawn into the wellbore giving higher temperatures. Greater temperatures produced a slightly higher total energy over the simulation at 2.66×10^{15} J.

4.3.4 Borehole radius

To investigate the effects of a slim borehole versus regular borehole, a range of well radii were used. Wellbores and well screen were modelled to be of equal diameter and had radii of 0.05 m, 0.15 m and 0.2 m. Although it is unlikely the former radius will be able to be drilled to depths >2 km (e.g., Adityatama et al., 2020), it is considered here from a theoretical viewpoint. Decreasing the radius resulted in a higher drawdown in the well, observed as a logarithmic relationship (Fig. 11b); however, this did not result in the cut-off criteria being met. Reducing the radii does have some added benefit – smaller radii result in slightly hotter production temperatures at the end of the simulation. The difference between the minimum and maximum production temperature was 1.53 °C. This may cause slim-boreholes to be of interest to single well schemes to further reduce the initial cost, whilst increasing heat loads.

4.4 Cluster analysis – highlighting risk

Although clear trends in the modelled data can be identified (4.1-4.3) with some analytics of single well performance over the lifetime, further quantitative analysis is required to determine the values which indicate risk. K-means cluster analysis was chosen to determine high or low risk data points and their respective parameters. The number of clusters must be chosen in advance using this method and was done so using the 'Elbow Method' where the within-cluster-sum of squared error (WCSS) was plotted against the number of clusters. As shown in figure 12a, the point where the WCSS shows the biggest drop between clusters is calculated as 5. The cluster analysis was performed by normalising the data using z-score normalisation before conducting K-means clustering (e.g., Lindsey et al., 2018). Cluster analysis was performed on both head and temperature in comparison to their cut-off points to determine groupings and therefore risk in relation to the pre-determined cut-offs.

Two distinct points sat as outliers and formed their own bins (clusters 1 and 2); these were for the lowest hydraulic conductivity and thermal gradient simulations, respectively (Fig. 12b). Both points class scenarios which were immediately un-feasible, reaching and surpassing the respective

cut-offs. Therefore, they were defined as high risk parameters. The other three clusters were focused around the bulk of the data. One cluster showed moderate-risk (cluster 3), one low-risk (cluster 4) and the last revolved around values in proximity to the base case scenario and was classed as moderate-low risk (cluster 5). The moderate-risk cluster incorporated two parameters which just surpassed the cut-off indicating risk; these were values with high flow rates and poor hydraulic conductivities. The other two values were within 100 m of the head cut-off and included values from the same risk groups. The low-risk solutions included the highest thermal gradient, the largest well screen and the well screen position located at the hottest part of the aquifer (i.e., the base). These parameters all increased the production temperatures, with some helping to mitigate drawdown. The final central cluster around the base case included other modelled values. The cluster centroids were: C1)1550 m, 79.02 °C, C2) 3300 m 56.97 °C, C3) 3003 m, 80.5 °C, C4) 3345 m, 87.43 °C, and C5) 3310 m, 79.09 °C.

4.5 Planning for risk - low hydraulic conductivities

Cluster analysis indicated variability in thermal gradient, hydraulic conductivity and production rate to pose the greatest threat to long-term maintenance of aquifer head and production temperature (Fig. 12b). Although different thermal gradients can dictate the initial temperature in a aquifer and therefore, the production temperature; it is difficult to alter these in single well schemes as the temperature may already be below the threshold for economic viability. The only way to alleviate this is by drawing in water at the base of the aquifer where the temperature will be greater, leading to the position of the well screen being influential. Low hydraulic conductivities, however, can be mitigated by using some of the low risk engineering parameters identified in figure 12b. The parameter that gave the highest head in the wellbore at the end of production was the well screen length. This and the production rate were, therefore, used to reduce the level of drawdown in the well. Although production rate was identified as moderate risk, as an engineering parameter it can be controlled, reduced and used to minimise drawdown.

Hydraulic conductivities of 0.01 m/day and 0.05 m/day were tested against both increased well screen lengths and decreased production rates. Well screen lengths were increased to have a penetration ratio of 50 % and 100 %, whilst production rates were reduced to 5 and 10 l/s. Reducing the production rate did help to reduce the amount of head depleted, but could not reduce drawdown sufficiently to make the lower hydraulic conductivity scenario viable (0.01 m/day). Increasing the screen length, however, did ensure that the lower hydraulic conductivity could be viable and the well head/temperature did not reach the cut-off.

When increasing the well screen length, drawdown was dramatically reduced. A 50 % well screen length reduced the amount of drawdown, leaving the final head in the wellbore at 3015 m for (0.01 m/day) and 3396 m (0.05 m/day) (Fig. 13a), far higher than that for the 10% penetration ratio (1554 m and 3104 m). For the same scenarios, final head levels for a fully penetrating well were 3230 m and 3439 m respectively (Fig. 13a). The difference in end production temperature for different hydraulic conductivities was minor and was noticeably more affected by different screen lengths (Fig. 13a). Although having a longer well screen is beneficial at increasing the lifetime and counteracting against poor hydraulic conductivities, it will be far more costly. It also has the ability to draw hotter water from deeper in the aquifer, increasing the energy output to 2.66 x 10^{15} J and 2.48 x 10^{15} J for full and 50 % penetration ratios.

When decreasing the production rate drawdown was slightly reduced. When modelling 10 l/s the final head in the wellbore was 2203m for (0.01 m/day) (Fig. 13b). Similarly, for slightly higher conductivity the wellbore head level increased to 3235m (0.05 m/day) (Fig. 13b). The final head levels for a production rate of 5 l/s were 2851 m (0.01 m/day) and 3367 m (0.05 m/day). It is key to note that the energy produced was greatly reduced to 1.51 x 10^{15} J and 6.57 x 10^{14} J, for 10 and 5 l/s respectively. Lowering the production rate does limit the amount of drawdown; however, it does substantially limit the amount of energy that can be produced. This is due to decreased production

temperatures and amount of fluid being produced. It also did not meet the cut-off for the lowest hydraulic conductivity.

The best solution to mitigate poor hydraulic conductivities may be to optimise a range of engineering characteristics, including production rate, position and length of well screen. Individually, increasing the well screen will help to maintain head, however, it may be more costly. Reduced production rates can also help to minimise drawdown, yet have the most influence on total energy extraction, as such in an ideal scenario this will be kept as high as possible.

5. Discussion

5.1 Parametric results

The results of this study show that in contrast to conventional hydrothermal development techniques (i.e., a doublet scheme) production temperature is likely to increase over the lifetime of a single production well when the penetrative interval is constrained to the upper portion of the aquifer. Groundwater flow was perpendicular- to hemispherical- towards the well screen at the top of the aquifer, which in turn causes upwelling and advective transport of heat from the base of the aquifer. Over the lifetime of the well, however, the change in production temperature was minimal and for all the scenarios modelled in this study temperature change is limited to a few degrees Celsius.

The hydrothermal modelling highlights the key risk parameters that influence single well production from deep geothermal systems are hydraulic conductivity, thermal gradient and production rate. Unsurprisingly, poor hydraulic conductivities create high drawdowns in the wellbore; however, this can be mitigated by altering the engineering parameters, such as the production rate, the position and length of the well screen. Although poor hydraulic conductivities can be mitigated, a reduction in total energy produced or initial increase in cost may be expected. It is also important to note that the initial aquifer temperature at the well screen is significant as small

changes in temperature were observed over the lifetime of a simulation. Therefore, an accurate subsurface temperature profile is required.

5.2 Limitations of the numerical modelling methodology

Multiple simulations were undertaken to test the effects of both geological and engineering parameters on single well geothermal production. Although some simplifications in aquifer conditions and modelling assumptions have been made in the study, the results may provide critical information (i.e., energy production, drawdown and production temperature) when assessing exploration and development of the basal Permian Collyhurst Sandstone Formation in the Cheshire Basin.

The modelling results showed porosity to have a minimal effect on the performance of a well. This is likely to be due to the limitation of the physical description of the modelling approach. A porosity-permeability relationship was not established; therefore, when testing the porosity in the parametric study a minor effect on temperature was observed, however, realistically this would affect groundwater flow and drawdown. Further consideration of this relationship for the Cheshire Basin must be undertaken to define the true impact of varying porosity. Additionally, the physical description could be improved to incorporate deformation and evolution of fluid density and viscosity under transient simulations to better represent the aquifer conditions. Although the average temperature change in the aquifer at the well screen is small (typically within 3°C), the incorporation of fluid density and viscosity as function of temperature and pressure will give more accurate results.

5.3 Coupling the 1D wellbore to a 3D aquifer

Simplification of the wellbore model to a series of 1D nodes allows accurate and efficient temperature prediction over the lifetime of a simulation. Losses in heat load along the borehole can be predicted, which can be minimised during the development well planning stage using the model.

The use of the finite-difference method allows this model to be easily reproduced on moderate performing computers. Additionally, the method of calculating head in the wellbore allows the numerical model to have a coarser grid size around the wellbore and faster computational times. The relatively high level of accuracy and small computational time also indicates the model to be useful in further multi-well regional scenarios for predicting long-term simulations.

5.4 Reliability and implications of regression analysis

Regression analysis of the numerical results can be used to give reliable estimates of both head and production temperature at the end of simulations without the need for complex numerical models. The regression models can also be used to extend the study outside the parameter range tested. The models indicate good accuracy in comparison to the numerical results with high R^2 values. All results other than the wellbore radius are above 0.91. Wellbore radius has a R^2 value of 0.866, suggesting the results of the regression model do not fit closely to the numerical with residuals for temperature reaching 0.24 °C.

In contrast, some regression fitted curves also have an R^2 of 1 or very close to. This indicates that the fitted curves account for the majority of the data (e.g., for thermal gradient and well screen position for production temperature, production rate for head). This is important as it shows that the regression curves can be used to accurately model production temperature or head at 25 years with a single calculation. Regression analysis is also useful as it can be used to determine the value for parameters which meet the cut-offs. For instance, the regression curves can be used to calculate the cut-offs for high risk parameters such as the thermal gradient to be 18.09 °C/km. It is worth stating that even though the results for well screen positioning do appear to have a strong fit, it is not necessarily reliable and may be a product of overfitting due to the use of a second-order polynomial trend line.

6. Conclusion

A sensitivity analysis of both geological and engineering parameters was undertaken for the Cheshire Basin to highlight operational risk in a single well system. Findings highlight that the key risks to consider are both geological and engineering, including thermal gradient, hydraulic conductivity and production rate. Thermal gradients can be estimated with some confidence using thermal gradients from existing nearby wells, but relies on detailed knowledge of the thermal regime in the subsurface. Conversely, it is difficult to estimate hydraulic conductivity at depth accurately. Core plugs, analogue offshore basins (East Irish Sea) and outcrop studies can give good estimations; however, the uncertainty at depth is unpredictable. Analysis undertaken highlights the negative effects of poor hydraulic conductivities can be mitigated by reducing the production rate and by increasing the length of well screen. Other engineering factors such as position of the well screen and radius of the wellbore (e.g., slim versus regular) can also aid in the alleviation of high drawdown during production caused by low hydraulic conductivities. Any development scheme must therefore be designed to incorporate the engineering factors outlined above to reduce the effects of poor aquifer hydro-physical parameters found during exploration ensuring productivity is sustainable for the desired lifetime of a well. Interestingly, the findings also highlight slim-boreholes (with smaller radii) have a slight positive impact on the total energy produced as fluid travels up the borehole faster, cooling at a slower rate. The negative effect of larger drawdown is also only minor, meaning a lower cost exploratory slim-borehole could be converted to an effective production well without further costly drilling of another development well.

The findings of this study are not only useful to well engineers, but also to town planners and those governing any district heating scheme in locations such as the Crewe area. The estimated variation in energy produced from the sensitivity analysis can be utilised in heat network planning, allowing demand to be matched to supply for best and worst case scenarios. The energy production can also be used by decision makers to decide the economic viability of any potential scheme. Typically, over a period of 25 years 2.37×10^{15} J of energy can be produced (for the base case), which accounts to 35 % of the maximum energy demand identified by Routledge et al. (2014). The

regression analysis can also provide a simplified equation to calculate wellbore heads, production temperatures and total energy without the need for detailed numerical modelling.

It is also important to note, that the key parameters influencing single well schemes are different to those in doublet and multi-well schemes. Whilst the main concern with injection-extraction doublet schemes is the time of thermal breakthrough, the primary focus of single well schemes is initial temperature and pressure depletion due to minimal temporal thermal changes. Thick aquifers, such as those in the Cheshire Basin, are more than capable of producing energy through single well partial penetration schemes for low energy demand schemes. However, ambiguity remains over the cost and environmental management of wastewater disposal, which must be the focus of future studies. For populous areas, such as Crewe, a multi-well or multi-method (both shallow and deep) geothermal scheme must be considered to meet the high demand and to account for the disposal of waste water. Further work on the basin should focus on establishing the true geology at depth in the Crewe area, particularly focusing on whether Carboniferous rocks are present.

Acknowledgements: C.S. Brown would like to thank the School of Geography, Geology and the Environment at Keele University for providing further support to the research conducted. He would also like to thank Lucy Smith for proof reading the manuscript, two anonymous reviewers and editor Jonathan Smith for their useful suggestions.

Funding: We would like to show appreciation to the Natural Environment Research Council (NERC grant reference number NE/M00998X/1) and Cheshire East Council for funding this research.

Availability of data and material: All data generated or analysed during this study are included in this published article.

References

Abdoh A, Cowan D, Pilkington M. 3D gravity inversion of the Cheshire Basin, *Geophysical Prospecting* 38, 999-1011. 1990. doi:10.1111/j.1365-2478.1990.tb01887.x

Adams J J, Bachu S. Equations of state for basin geofluids: algorithm review and intercomparison for *brines. Geofluids*, 2: 257–271. 2002. doi:10.1046/j.1468-8123.2002.00041.x

Adityatama, D.W., Purba, D., Muhammad, F., Agustino, V., Wiharlan, H. and Pasmeputra, K.K., Slim Hole Drilling Overview for Geothermal Exploration in Indonesia: Potential and Challenges. PROCEEDINGS, 45th Workshop on Geothermal Reservoir Engineering Stanford University, Stanford, California, February 10-12, 2020.

Al-Khoury R, Bonnier P G, Brinkgreve B J. Efficient finite element formulation for geothermal heating systems. Part I: steady state. *International Journal for Numerical Methods in Engineering* 63, 988–1013. 2005. doi: 10.1002/nme.1313

Al-Khoury R, Bonnier P G. Efficient finite element formulation for geothermal heating systems. Part II: transient. *International Journal for Numerical Methods in Engineering* 67, 725–745. 2006 doi: 10.1002/nme.1662

Allen D J, Gale I N, Price M. Evaluation of the Permo-Triassic sandstones of the UK as geothermal aquifers. *Hydrogeol. Ill Serv. Mall Memoires 18th Congr*. Int. Assoc. Hydrogcologists Camb. 1985.

Allen D J, Brewerton L J, Coleby L M, Gibbs B R, Lewis M A, MacDonald A M, Wagstaff S J, Williams A T. The physical properties of major aquifers in England and Wales. 1997. British Geological Survey Technical Report WD/97/34. Environment Agency R&D Publication 8. BGS, Keyworth.

Ambrose K, Hough E, Smith N J P, Warrington G. Lithostratigraphy of the Sherwood Sandstone Group of England, Wales and south-west Scotland. Br. Geol. Surv. Res. Rep. 2014

Anderson M P, Woessner W W, Hunt R J. Applied groundwater modeling: simulation of flow and advective transport. Academic press; 2015.

Atkins. Deep Geothermal Review Study. Final Report for the Department of Energy & Climate Change (DECC). 2013.

Barker J A, Downing R A, Gray D A, Findlay J, Kellaway G A, Parker R H, Rollin K E. Hydrogeothermal studies in the United Kingdom. *Quarterly Journal of Engineering Geology and Hydrogeology*, 33(1), pp.41-58. 2000. doi:10.1144/qjegh.33.1.41

Batzle M, Wang Z. Seismic properties of pore fluids. *Geophysics* 57 (11), 1396–1408. 1992. doi: 10.1190/1.1443207

BGS. Temperature and thermal properties. A report by the British Geological Survey. BGS Report No: GR_999999/1. 2011.

Brown, C.S. *Modelling, characterisation and optimisation of deep geothermal energy in the Cheshire basin.* PhD thesis, University of Birmingham. 2020.

Brown, C.S., Cassidy, N.J., Egan, S.S. and Griffiths, D. Numerical modelling of deep coaxial borehole heat exchangers in the Cheshire Basin, UK. *Computers & Geosciences*, *152*, p.104752. 2021

Burley A J, Smith I F, Lee M K, Burgess W G, Edmunds W M, Arthur M J, Bennett J R P, Carruthers R M, Downing R A, Houghton M. Preliminary Assessment of the Geothermal Potential of the United Kingdom, in: Strub, A.S., Ungemach, P. (Eds.), *Advances in European Geothermal Research*. Springer Netherlands, pp. 99–108. T 1980.

Busby J P. Geothermal prospects in the United Kingdom. Presented at the World Geothermal 924 Congress 2010, Bali, Indonesia. 2010.

Busby J, Kingdon A, Williams J. The measured shallow temperature field in Britain. *Quarterly Journal of Engineering Geology and Hydrogeology*, 44(3), pp.373-387. 2011. doi:10.1144/1470-9236/10-049

Busby J. Geothermal energy in sedimentary basins in the UK. *Hydrogeology journal*, 22(1), pp.129-141. 2014. doi:10.1007/s10040-013-1054-4

Brons and Marting. The effect of restricted fluid entry on well productivity. Journal of Petroleum Technology. Vol. 13, no. 2, 172-174. 1961. doi: 10.2118/1322-G-PA

Cai Z, Ofterdinger U. Numerical assessment of potential impacts of hydraulically fractured B owland S hale on overlying aquifers. Water Resources Research. 2014 ;50(7):6236-59.

Crooijmans R A, Willems C J L, Nick H M, Bruhn D F. The influence of facies heterogeneity on the doublet performance in low-enthalpy geothermal sedimentary reservoirs. *Geothermics*, 64, pp.209-219. 2016. doi:10.1016/j.geothermics.2016.06.004

Downing R A, Allen D J, Barker J A, Burgess W G, Gray D A, Price M, Smith I F. Geothermal exploration at Southampton in the UK: a case study of a low enthalpy resource. *Energy exploration & exploitation*, 2(4), 327-342. 1984.

Downing R A, Gray D A. Geothermal Energy The potential in the United Kingdom. BGS, 941 National Environment Research Council. 1986.

Energie-Cités. Geothermal Energy District heating scheme Southampton (United Kingdom). Case study prepared with the City of Southampton. 2001. https://geothermalcommunities.eu/assets/elearning/5.13.SOUTH_EN.PDF

Evans D J, Rees J G, Holloway S. The Permian to Jurassic stratigraphy and structural evolution of the central Cheshire Basin. J. Geol. Soc. 150, 857–870. 1993. doi:10.1144/gsjgs.150.5.0857

ETB. The Engineering Toolbox. 2017. [http://www.engineeringtoolbox.com/water-thermal-properties-d_162.html]. Website accessed on 06/03/2017.

Farr, G., Busby, J., Wyatt, L., Crooks, J., Schofield, D.I. and Holden, A., 2021. The temperature of Britain's coalfields. *Quarterly Journal of Engineering Geology and Hydrogeology*, *54*(3).

Geiser J. Iterative operator-splitting methods with higher-order time integration methods and applications for parabolic partial differential equations. *Journal of Computational and Applied Mathematic*s, 217(1), pp.227-242. 2008. doi.10.1016/j.cam.2007.06.028

Gibson W. Upper Coal Measures of the Midlands. 57, 251 – 266. 1901.

Glennie K W. Permian and Triassic rifting in northwest Europe. Geol. Soc. Lond. Spec. Publ. 91, 1–5. 1995. doi:10.1144/GSL.SP.1995.091.01.01

Gluyas, J.G., Adams, C.A., Busby, J.P., Craig, J., Hirst, C., Manning, D.A.C., McCay, A., Narayan, N.S., Robinson, H.L., Watson, S.M. and Westaway, R., 2018. Keeping warm: a review of deep geothermal potential of the UK. *Proceedings of the Institution of Mechanical Engineers, Part A: Journal of Power and Energy*, *232*(1), pp.115-126.

Griffiths K J, Shand P, Ingram J. Baseline Report Series: 8. The Permo-Triassic Sandstones of Manchester and East Cheshire British Geological Survey Commissioned Report No. CR/03/265N. 2003.

Griffiths, K.J., Shand, P. and Ingram, J., 2005. Baseline report series. 19, the Permo-Triassic sandstones of Liverpool and Rufford.

Halford K J, Hansen R T. User Guide for the Drawdown-Limited, Multi-Node Well (MNW) Package for the U.S. Geological Survey's Modular Three-Dimensional Finite Difference Ground-Water Flow Model, Versions MODFLOW-96 and MODFLOW-2000 (Vol. 2, No. 293). Us Department of the Interior, US Geological Survey. 2002.

Hantush M S. Drawdown around a partially-penetrating well. J. Hydraul. Div., Proc. ASCE, 87(HY4): 83-98. 1961.

Hantush M S. Aquifer tests on partially penetrating wells, American Society of Civil Engineers. Trans. Vol 127. Part 1, 284-308. 1962.

Hirst C M, Gluyas J G, Adams C A, Mathias S A, Bains S, Styles P. UK Low Enthalpy Geothermal Resources: the Cheshire Basin. Proc. World Geotherm. Congr. 2015.

Hirst, C M. *The geothermal potential of low enthalpy deep sedimentary basins in the UK*. Diss. Durham University, 2017.

Howell, L., Brown, C.S. and Egan, S.S. Deep geothermal energy in northern England: Insights from 3D finite difference temperature modelling. *Computers & Geosciences*, *147*, p.104661. 2021.

Huisman L. Ground water recovery. Winchester Press, New York, p. 131. 1972.

Konikow L F, Hornberger G Z, Halford K J, Hanson R T. Revised multi-node well (MNW2) package for MODFLOW ground-water flow model: U.S. Geological Survey Techniques and Methods 6–A30, 67 p. 2009.

Kozeny J. Theorie und berechnung der brunnen: Wasserkraft und Wasserwirtschaft, v. 28. 1933.

Lindsey, C.R., Neupane, G., Spycher, N., Fairley, J.P., Dobson, P., Wood, T., McLing, T. and Conrad, M. Cluster analysis as a tool for evaluating the exploration potential of Known Geothermal Resource Areas. *Geothermics*, *72*, pp.358-370. 2018.

Lund J W, Freeston D H, Boyd T L. Direct utilization of geothermal energy 2010 worldwide review. Geothermics, 40(3), pp.159-180. 2011.

Manning, D.A.C., Younger, P.L., Smith, F.W., Jones, J.M., Dufton, D.J. and Diskin, S., 2007. A deep geothermal exploration well at Eastgate, Weardale, UK: a novel exploration concept for low-enthalpy resources. *Journal of the Geological Society*, *164*(2), pp.371-382.

Mikkelsen P W, Floodpage J B. The hydrocarbon potential of the Cheshire Basin, Geological Society, London, Special Publications, v. 124, no. 1, p. 161-183. 1997. doi:10.1144/GSL.SP.1997.124.01.10

Naylor H, Turner P, Vaughan D J, Boyce A J, Fallick A E. Genetic studies of red bed mineralization in the Triassic of the Cheshire Basin, northwest England. J. Geol. Soc. 146, 685–699. 1989. doi:10.1144/gsjgs.146.4.0685

Ozbek H, Phillips S L. Thermal Conductivity of Aqueous NaCl Solutions from 20Ċ to 330Ċ. Department of Energy, Lawrence Berkeley Laboratory. 1979.

Pasquali R, O'Neill N, Reay D, Waugh T. The geothermal potential of Northern Ireland. Proc. World Geotherm. Congr. 2010 Bali Indones. 2010.

Peaceman, D.W., 1983, Interpretation of well-block pressures in numerical reservoir simulation with nonsquare grid blocks and anisotropic permeability: Society of Petroleum Engineers Journal, v. 23, no. 3, p. 531–543.

Pharaoh, T.C., Gent, C.M.A., Hannis, S.D., Kirk, K.L., Monaghan, A.A., Quinn, M.F., Smith, N.J.P., Vane, C.H., Wakefield, O. and Waters, C.N., 2019. An overlooked play? Structure, stratigraphy and hydrocarbon prospectivity of the Carboniferous in the East Irish Sea–North Channel basin complex. *Geological Society, London, Special Publications*, *471*(1), pp.281-316.

Plant J A, Jones D G, Haslam H W. The Cheshire Basin - Basin evolution, fluid movement & mineral resources in a Permo-Triassic rift setting. Br. Geol. Surv. Nottm. UK. 1999.

Powell J H, Chisholm J I, Bridge D, Rees J G, Glover B W, Besly B M. Stratigraphical framework for Westphalian to Early Permian red-bed successions of the Pennine Basin British. Geol. Surv. Res. Rep. 2000.

Price M, Allen D J. The use of pumping tests to evaluate a geothermal reservoir-the Triassic sandstones at Marchwood, Southampton. Proceedings of the Institution of Civil Engineers, 76(3), 697-711. 1984.

Prickett T A. Designing pumped well characteristics into electric analog models. Groundwater, 5(4), pp.38-46. 1967. doi:10.1111/j.1745-6584.1967.tb01625.x

Rollin K E, Kirby G A, Rowley W J, Buckley D K. Atlas of Geothermal Resources in Europe: UK Revision. Technical Report WK/95/07, British Geological Survey, Keyworth. 1995.

Rosen M A, Koohi-Fayegh S. Geothermal energy: Sustainable heating and cooling using the ground. John Wiley & Sons. 2017.

Routledge K, Williams J, Lehdonvirta H, Kuivala J-P, Fagerstrom O/ Heat Network Mapping for Leighton West. A report prepared for Cheshire East Council. Report number: 298-692. 2014.

Rowley E, White N. Inverse modelling of extension and denudation in the East Irish Sea and surrounding areas. Earth Planet. Sci. Lett. 161, 57–71. 1998. doi:10.1016/S0012-821X(98)00137-X

Ruffell A, Shelton R. The control of sedimentary facies by climate during phases of crustal extension: examples from the Triassic of onshore and offshore England and Northern Ireland. J. Geol. Soc. 156, 779–789. 1999. doi:10.1144/gsjgs.156.4.0779

Rushton, K.R. Groundwater hydrology: conceptual and computational models. John Wiley & Sons. 2003.

Sachse, A., Rink, K., He, W., Kolditz, O. OpenGeoSys-Tutorial: computational hydrology I: groundwater flow modeling. Springer. 2015.

Saeid S, Al-Khoury R, Barends F. An efficient computational model for deep low-enthalpy geothermal systems. Computers & geosciences, 51, pp.400-409. 2013. doi:10.1016/j.cageo.2012.08.019

Saeid S, Al-Khoury R, Nick H M, Hicks M A. A prototype design model for deep low-enthalpy hydrothermal systems. Renew. Energy 77, 408–422. 2015. doi:10.1016/j.renene.2014.12.018

Smith N T. The Carboniferous to Mesozoic structural and stratigraphic evolution of the Cheshire basin. Unpublished PhD. 1998.

Smith, M. Southampton energy scheme. Proceedings World Geothermal Congress, Kyushu - Tohoku, Japan, May 28 - June 10, 2000.

Spiegelman M. Myths and methods in modeling. Columbia University Course Lecture Notes. 2000.

Sternberg Y M. Efficiency of Partially Penetrating Wells. Ground Water., Vol. 11, No. 3. 1973. doi: 10.1111/j.1745-6584.1973.tb02967.x

Thiem G. Hydrologische Methoden. Gebhardt, Leipzig. 1906.

UKOGL. UK Onshore Geophysical Library. 2016. [https://ukogl.org.uk/map/] Accessed on the 08/09/2016.

University of Birmingham, 1984. Saline Groundwater Investigation. Phase 2 – North Merseyside. Final Report to North West Water Authority.

Van Genuchten, M. T., Alves, W. J. Analytical solutions of the one-dimensional convective dispersive solute transport equation (No. 157268). United States Department of Agriculture, Economic Research Service. 1982.

Verhoeven, R., Willems, E., Harcouët-Menou, V., De Boever, E., Hiddes, L., Op't Veld, P. and Demollin, E., 2014. Minewater 2.0 project in Heerlen the Netherlands: transformation of a geothermal mine water pilot project into a full scale hybrid sustainable energy infrastructure for heating and cooling. *Energy Procedia*, *46*, pp.58-67.

Waples D W, Waples J S. A review and evaluation of specific heat capacities of rocks, minerals, and subsurface fluids. Part 1: Minerals and nonporous rocks. Natural resources research, 13(2), pp.97-122. 2004. doi:10.1023/B:NARR.0000032647.41046.e7

Watson, S.M., Westaway, R. and Falcone, G., 2019. A Review of Deep Geothermal Energy and Future Opportunities in the UK. In *Proc. European Geothermal Congress*.

Watson, S.M., Falcone, G. and Westaway, R., 2021. Repurposing hydrocarbon wells for geothermal use in the UK: A preliminary resource assessment.

Westaway, R., 2018. Deep geothermal single well heat production: critical appraisal under UK conditions. *Quarterly Journal of Engineering Geology and Hydrogeology*, *51*(4), pp.424-449.

Wu H, Fu P, Morris J P, Settgast R R, Ryerson F J and Team E C. A Numerical Scheme to Reduce Numerical Diffusion for Advection-Dispersion Modeling: Validation and Application. In 44th Workshop on Geothermal Reservoir Engineering. 2019

Younger, P.L. and Manning, D.A., 2010. Hyper-permeable granite: lessons from test-pumping in the Eastgate Geothermal Borehole, Weardale, UK. *Quarterly Journal of Engineering Geology and Hydrogeology*, *43*(1), pp.5-10.

Younger, P.L., Manning, D.A., Millward, D., Busby, J.P., Jones, C.R. and Gluyas, J.G., 2016. Geothermal exploration in the Fell Sandstone Formation (Mississippian) beneath the city centre of Newcastle upon Tyne, UK: the Newcastle Science Central deep geothermal borehole. *Quarterly Journal of Engineering Geology and Hydrogeology*, *49*(4), pp.350-363.

Appendix: Nomenclature

Symbol	Parameter	Units
t	Time	seconds
λ	Thermal conductivity	W/m/°C
T	Temperature	°C
$\emptyset$	Porosity	%
C	Specific heat capacity	J/kg °C
ρ	Density	kg /m^3
α	Thermal diffusivity	m^2/s
R_d	Retardation factor	-
K	Hydraulic conductivity	m/s
v	Darcy velocity	m/s
Ss	Storage coefficient	-
h	Hydraulic head	m
Pr	Penetration ratio	-
PC	Pricketts penetration constant for additional drawdown	-
dV	Volume	m^3
u	Fluid velocity in the pipe	m/s
b_{pg}	Reciprocal of thermal resistance between pipe and grout	-
dS_{pg}	Contact area between pipe and grout	m²
Q	Flow rate	m^3/s
W	Source or sink	m/s
rw	Radius of the well in the aquifer (screened interval)	m
re	Extrapolated radius	m

Tables:

Parameters	
Production rate (l/s)	15
Initial thermal gradient (°C/km)	25
Surface temperature (°C)	10
Thermal conductivity (W/m/°C)	2.12 UCB / 3.41 R / 0.67 F
Specific heat capacity (J/kg °C)	950 UCB / 1100 R / 4200 F
Density (kg/m^3)	2720 UCB / 2450 R / 1024.7 F
Porosity (%)	15
Hydraulic conductivity (m/d)	0.1
Salinity (g/l)	80

Table 1. Base case parameters used in this study, from (Downing and Gray, 1986; Burley et al., 1980; Allen et al., 1997; Waples and Waples, 2004; ETB, 2017). Upper confining bed = UCB, aquifer = R and fluid = F.

Parameters	
Radius of well screen (m)	0.106
Thermal conductivity (W/m/°C)	43 P/ 2.7 G
Specific heat capacity (J/kg °C)	1250 G
Density (kg/m^3)	1600 G
Pipe thickness (m)	0.02
Grout thickness (m)	0.04

Table 2. Borehole parameterisation of both materials and radius to test the thermal and pressure effects, from (Allan, 1997; ETB, 2017; Rosen and Koohi-Fayegh, 2017). Pipe = P and grout = G.

Case	S1	S2	S3
Porosity (%)	10	20	30
Hydraulic conductivity (m/day)	0.01	0.03	0.05
Aquifer thickness (m)	630	840	770
Thermal gradient (°C/km)	28	23	17
Thermal conductivity (W/m/°C)	2	4	5
Production rate (l/s)	20	30	40
Well screen position (km)	2.94-3.01	3.29-3.36	3.43-3.5
Well screen length (m)	700	280	140
Radius of wellbore (cm)	5	15	20

Table 3. Parameter alterations used in sensitivity analysis.

Figures

Figure 1. Map of the UK highlighting key Mesozoic Basins and Granitic intrusions (after Downing and Gray, 1986; Busby, 2010; Pasquali et al., 2010). Low-enthalpy HSAs are confined to Mesozoic basins, whilst hot dry rock prospects are related to high-heat flow igneous intrusions. The brown basins are other minor Mesozic basins in the UK where depth data has not been listed for this study.

Figure 2. (a) Example discretised domain for aquifer. Vertical spacing is uniform and is set at 14 m, whilst the horizontal spacing increases away from the well screen (thick black line) at an expansion factor of 1.2 – 1.5. Mercia Mudstone Group = MMG, Sherwood Sandstone Group = SSG and Manchester Marl Formation is MM fm. (b) The interpreted geological model in 2D (formation boundaries obtained from structural maps from Downing and Gray, (1986)). Minimum spacing around the wellbore of 8 m.

Figure 3. (a) Geological outcrop map of the Cheshire Basin (after Plant et al., 1999; Hirst et al., 2015; UKOGL, 2016). Permo-Triassic sandstones are the dominant infill (Appleby and Sherwood Sandstone Groups), capped by a sequence of thick insulating mudstones (Mercia Mudstone and Lias Groups). (b) Schematic of the tectonic history of the basin and (c) cross section of the basin (both modified after Plant et al., 1999), with the potential extent of Carboniferous strata in the subsurface.

Figure 4. Example nodal domain showing wellbore radius, equivalent radius and nodal spacing (e.g., after Halford and Hanson, 2002).

Figure 5. Comparison between the analytical solution for partially penetrative schemes (modified Theis) and numerical finite-difference method for drawdown in the wellbore.

Figure 6. (a) Comparison between the analytical solution for heat flow in a borehole and finite-difference method. (b) The difference in head (root mean squared error - RMSE) and the mean average percentage error (MAPE) between the analytical and numerical solution.

Figure 7. (a) 2D cross slices through the entire subsurface after 25 years, (b) head, aquifer temperature as an average across the well screen and production temperature v time, (c) Temperature distributions in the wellbore after 6 hours, 12 hours, 1 year, 10 years and 20 years, (d) changes in temperature in the confining beds around the wellbore at the surface level (S.L), 1500 m and 2700 m.

Figure 8. Production temperature at the end of the 25 year simulation for (a) porosity, (b) thermal conductivity and (c) aquifer thickness. (d) Production temperature and total energy for the thermal gradient at the end of the simulation. Numerical data and calculated regression curves shown as black asterisks and dashed lines, respectively.

Figure 9. Production temperature and hydraulic head at the end of the 25 year simulation for hydraulic conductivity. Numerical data and calculated regression curves shown as black asterisks and lines, respectively. Note the black data points correspond to both axis showing the respective production temperatures and heads.

Figure 10. Production temperature and hydraulic head at the end of the 25 year simulation for (a) well screen position and (b) production rate. (c)Total energy produced during the simulation for well screen position and production rate. Numerical data and calculated regression curves shown as black asterisks and lines, respectively.

Figure 11. Production temperature and hydraulic head at the end of the 25 year simulation for (a) well screen length and (b) wellbore radius. Numerical data and calculated regression curves shown as asterisks and lines, respectively.

Figure 12. Cluster analysis of all modelled data at the end of the simulation. (a) Scree plot of the within-cluster-sum of squared error (WCSS) and the number of clusters. (b) Production temperature and head k-means cluster plot, highlighting cut-offs and key parameters.

Figure 13. Production temperature and head variations with time during the depletion phase investigating the mitigation of hydraulic conductivities with varying length of the well screen (a) and production rates (b). There are two clear temperature profiles in both, respective of the engineering parameter. Although minor changes in aquifer temperature are caused they do not strongly influence the production temperature.

Figure 1

Figure 2

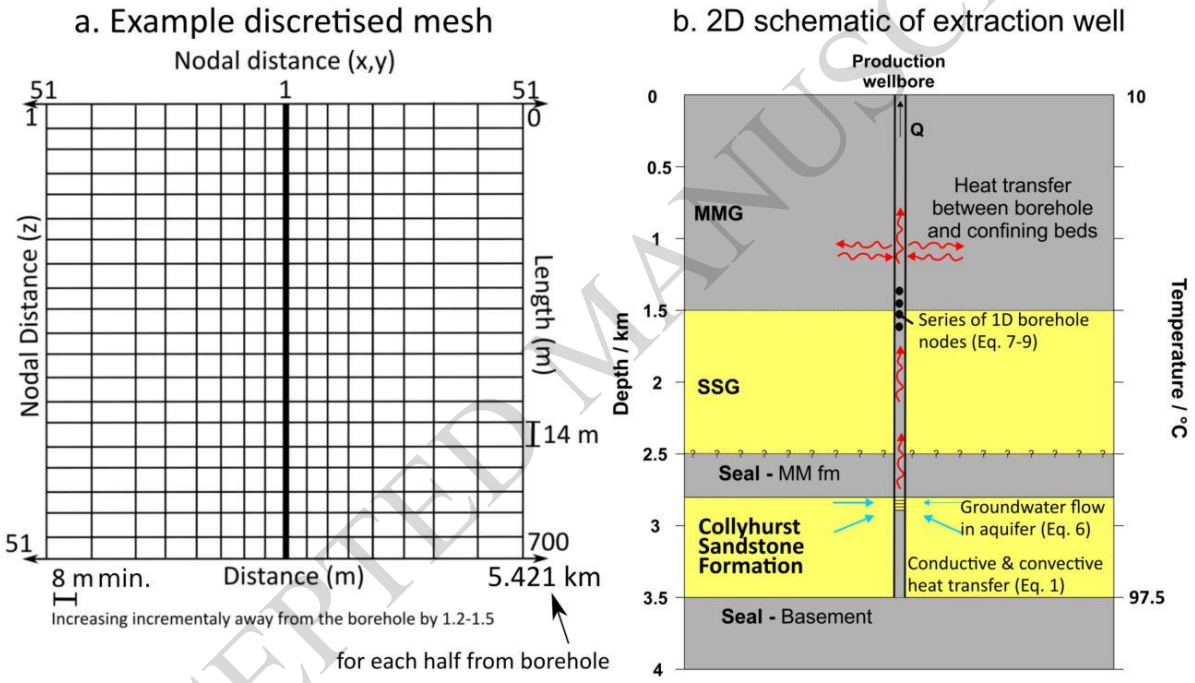

Figure 3

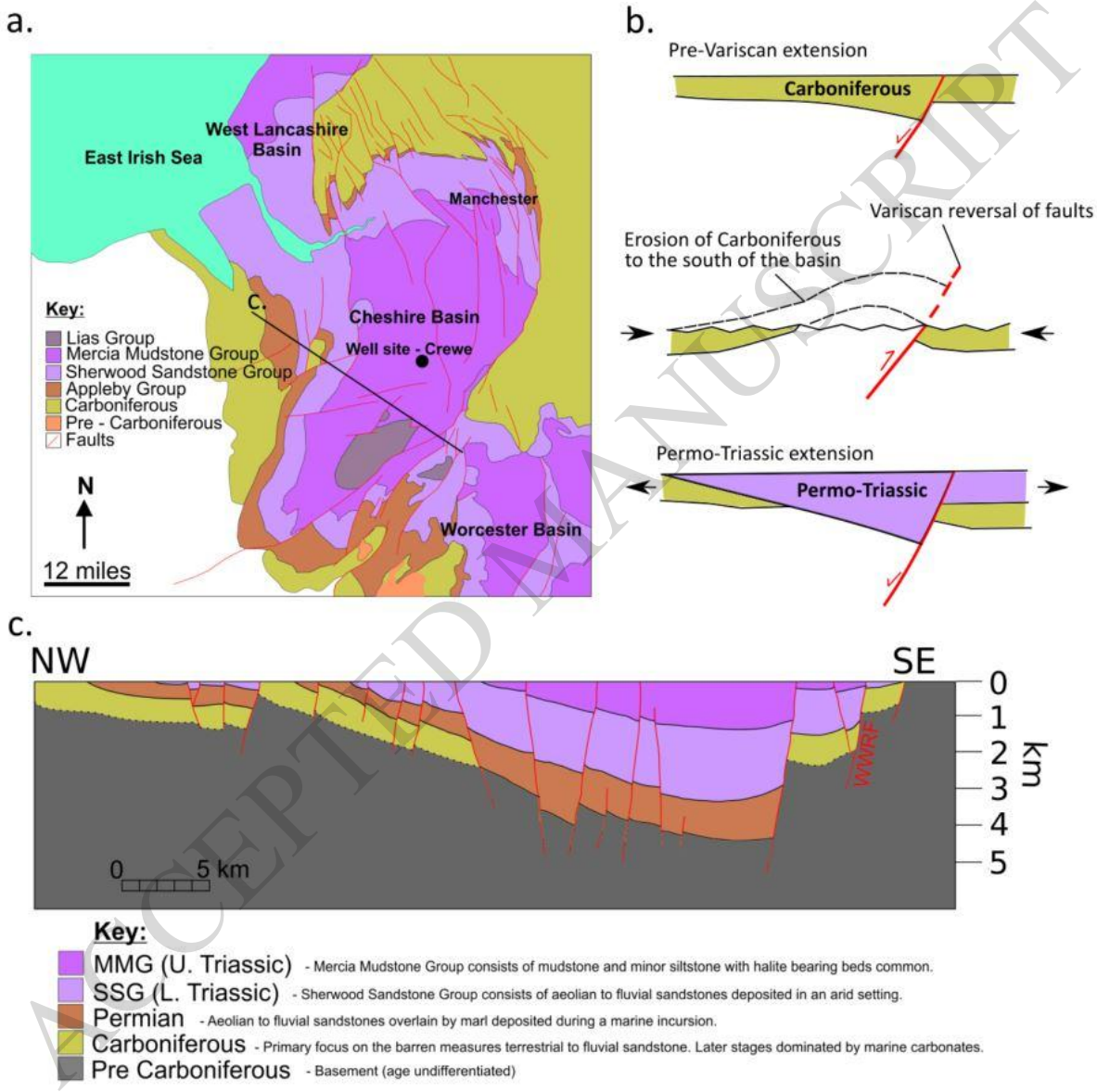

Figure 4

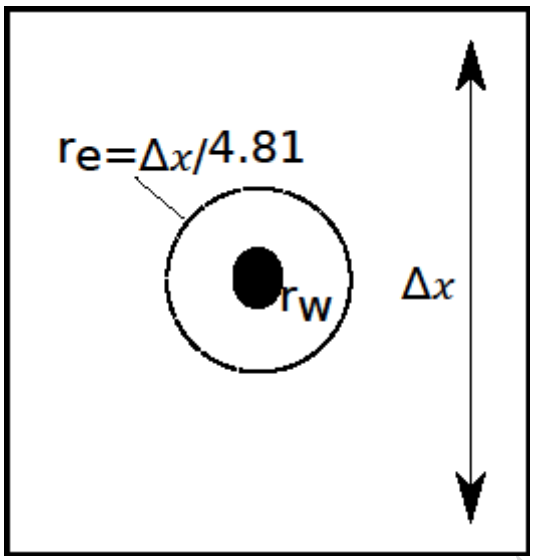

Figure 5

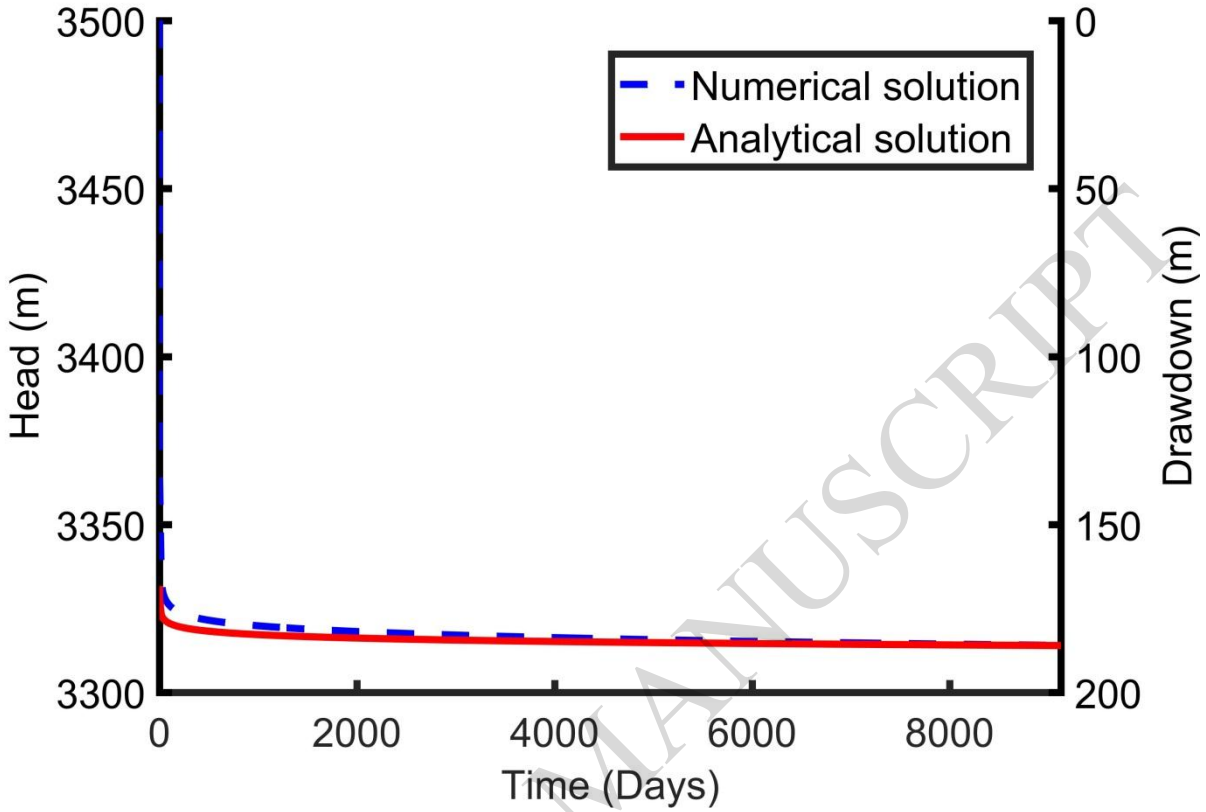

Figure 6

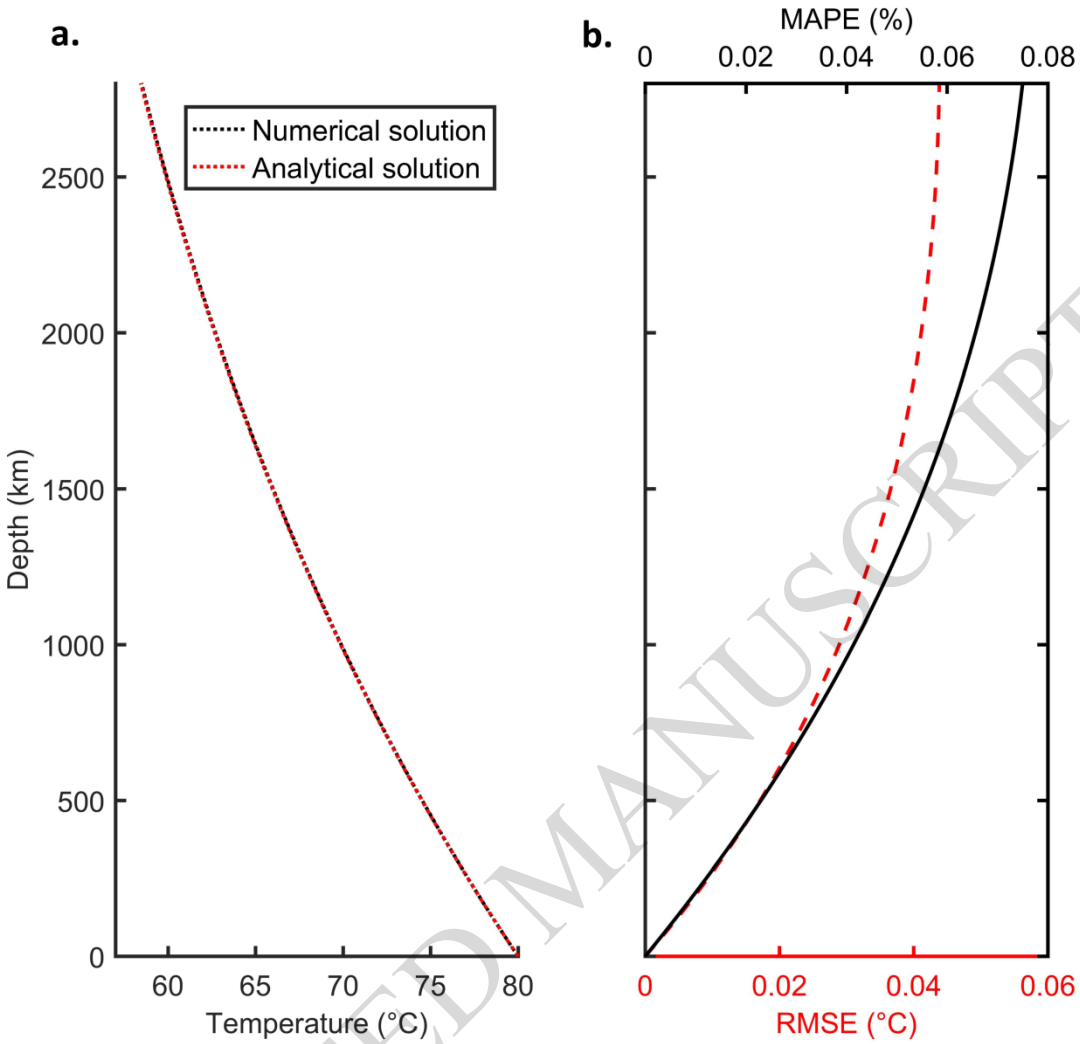

Figure 7

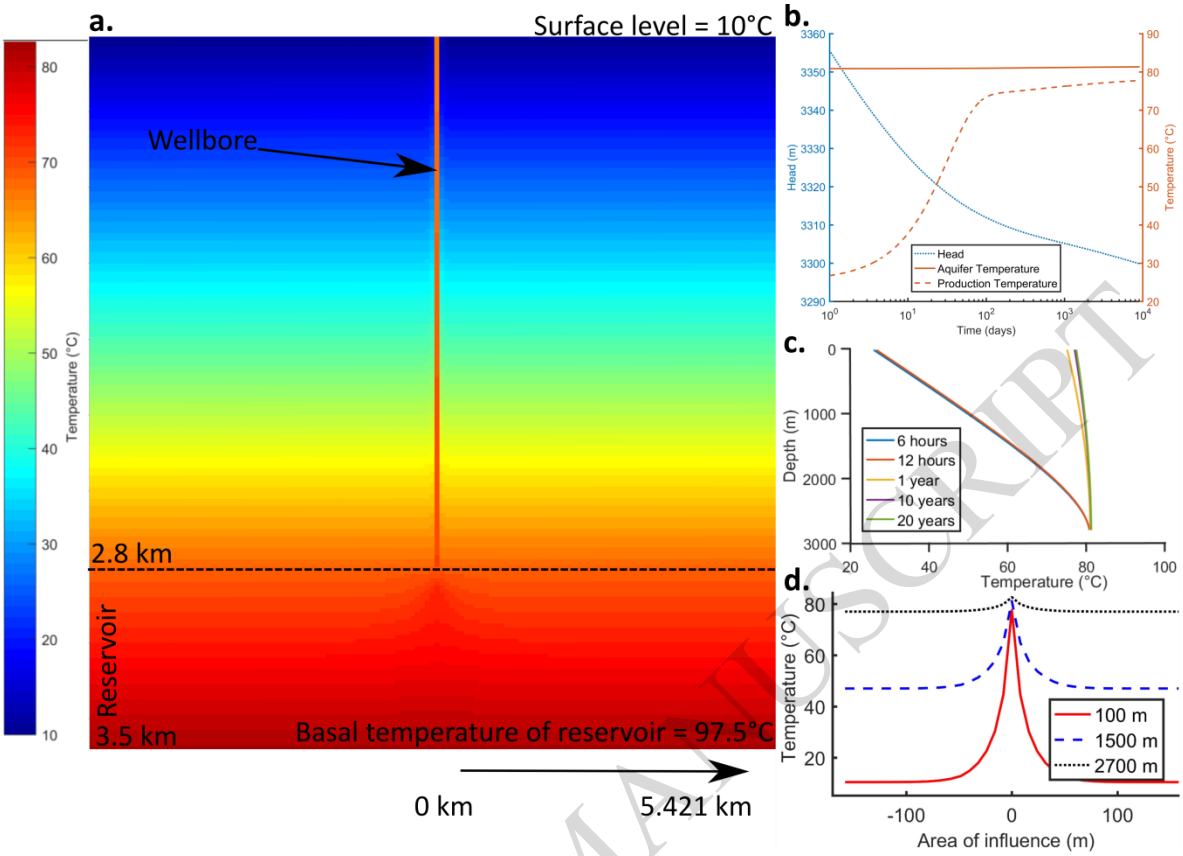

Figure 8

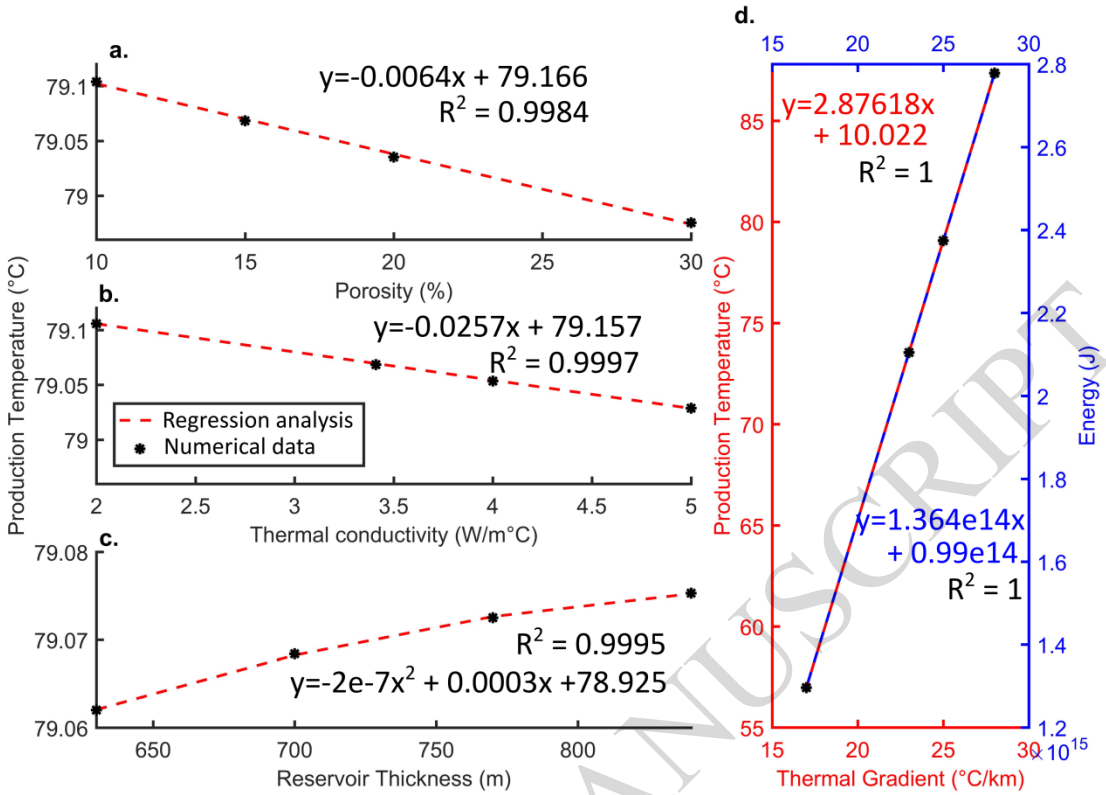

Figure 9

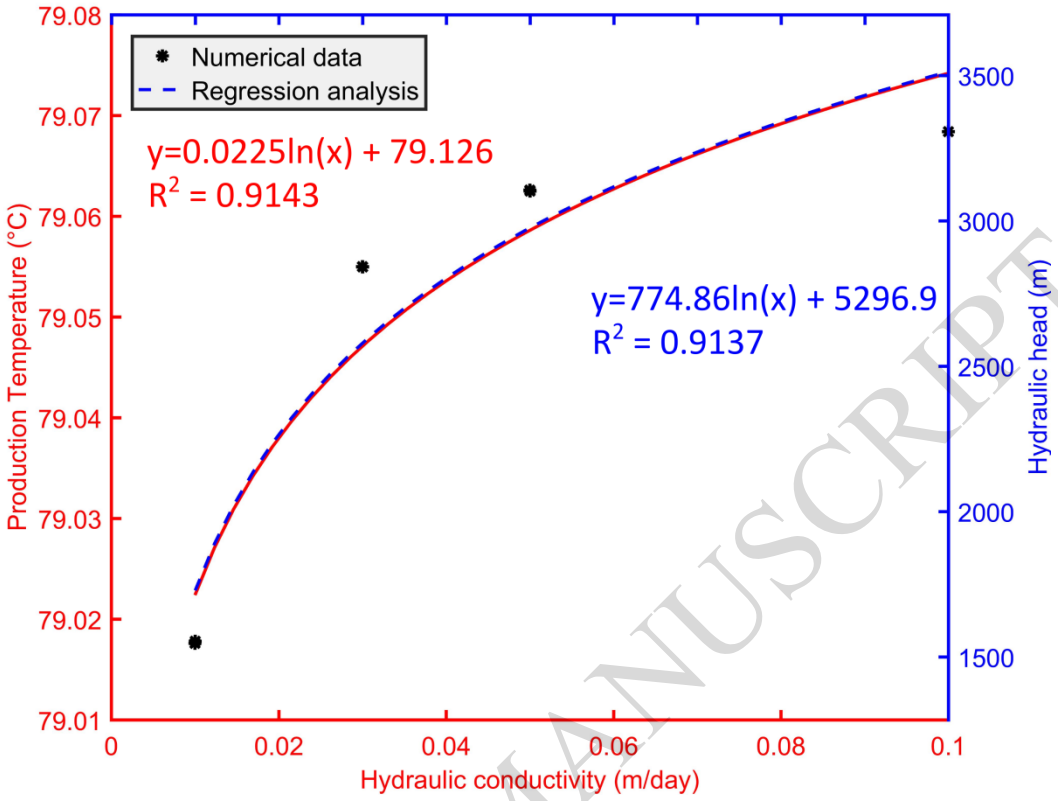

Figure 10

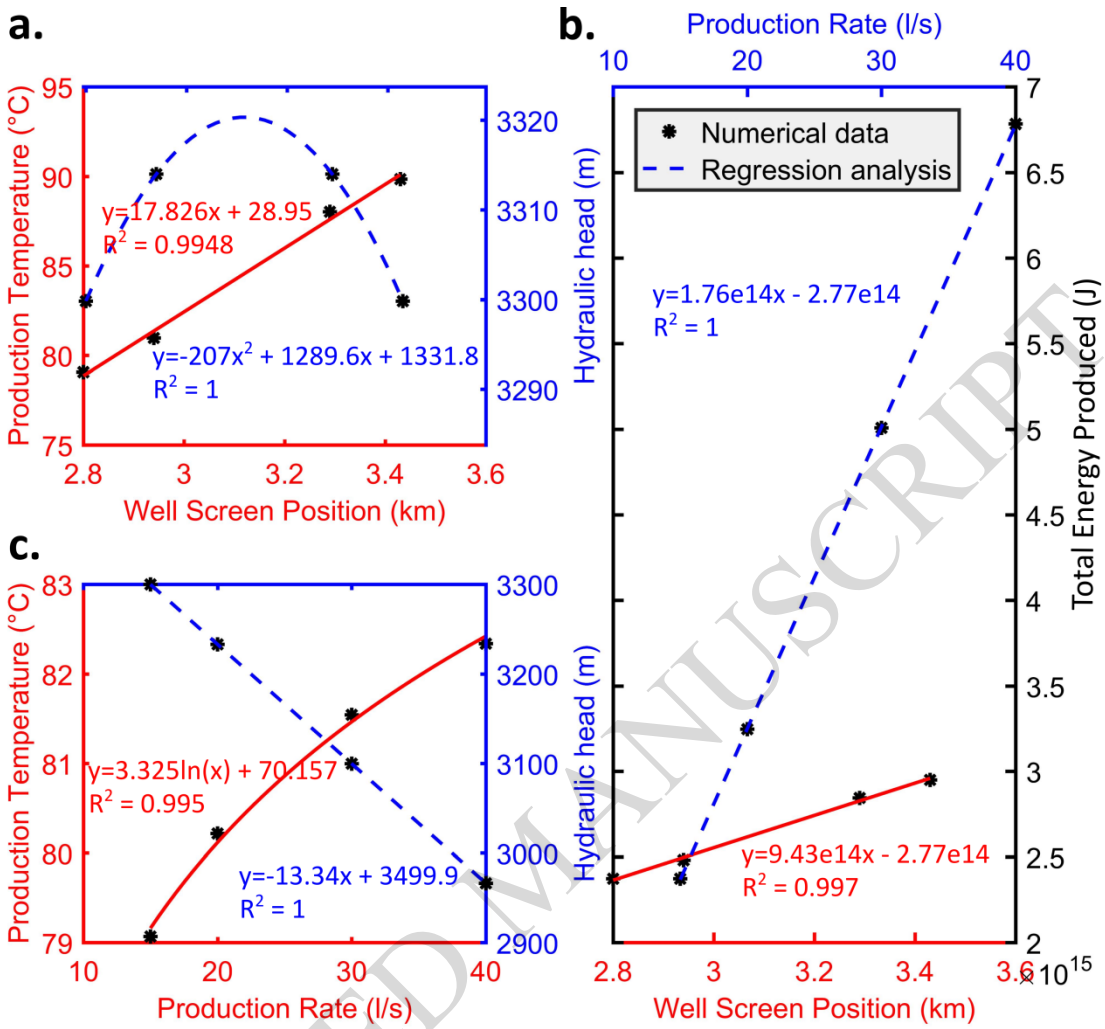

Figure 11

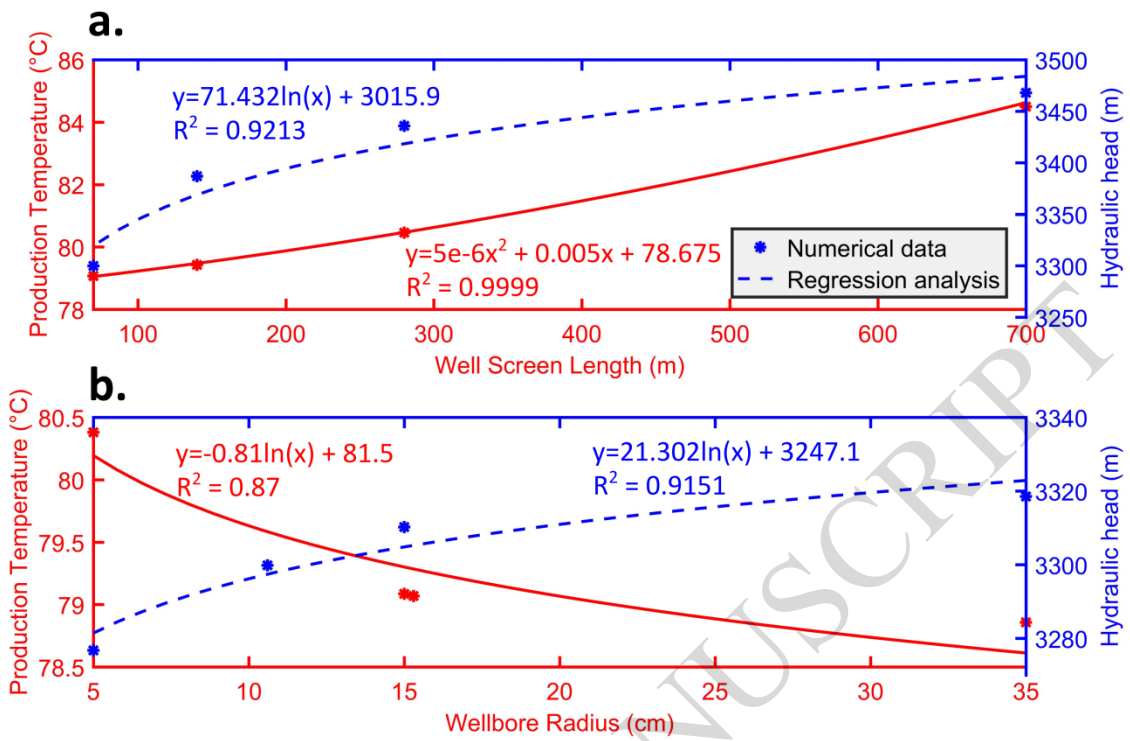

Figure 12

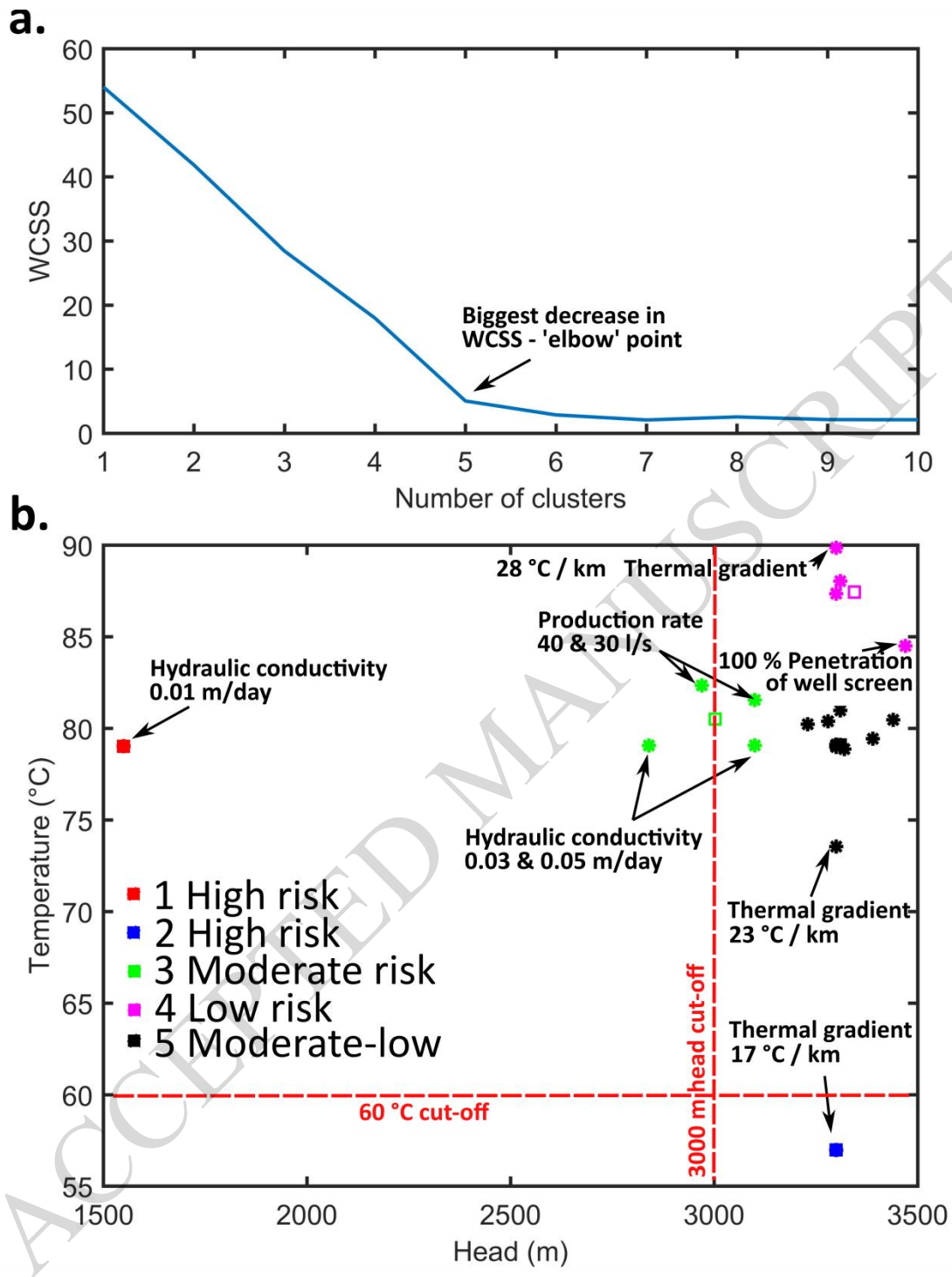

Figure 13